Electronic ISSN: 1309-0267

I
J
E
A
S

International Journal of Engineering & Applied Sciences

IJEAS

Volume 12, Issue 3
2020

Published by Akdeniz University

Editorial Board

(The name listed below is not Alphabetical or any title scale)

Abstracting & Indexing

IJEAS provides unique DOI link to every paper published.

Editorial Scope

The journal presents its readers with broad coverage across some branches of engineering and science of the latest development and application of new solution algorithms, artificial intelligent techniques innovative numerical methods and/or solution techniques directed at the utilization of computational methods in solid and nano-scaled mechanics.

International Journal of Engineering & Applied Sciences (IJEAS) is an Open Access Journal

International Journal of Engineering & Applied Sciences (IJEAS) publish original contributions on the following topics:

Numerical Methods in Solid Mechanics

Nanomechanic and applications

Microelectromechanical systems (MEMS)

Vibration Problems in Engineering

Higher order elasticity (Strain gradient, couple stress, surface elasticity, nonlocal elasticity) Applied Mathematics

IJEAS allows readers to read, download, copy, distribute, print, search, or link to the full texts of articles.

CONTENTS

International Journal of Engineering & Applied Sciences (IJEAS)
Vol. 12, Issue 3 (2020) 88-98
http://dx.doi.org/10.24107/ijeas.790858
Int J Eng Appl Sci 12(3) (2020) 88-98

Static Analysis of a Fiber Reinforced Composite Beam Resting on Winkler-Pasternak Foundation

Şeref Doğuşcan Akbaş

Bursa Technical University, Department of Civil Engineering, Bursa, Turkey.
E-mail address: serefda@yahoo.com

ORCID numbers of author:
0000-0001-5327-3406

Received date: 05.09.2020
Accepted date: 18.11.2020

Abstract

This paper presents static analysis of a simply supported beam made of fiber reinforced composite material resting on elastic foundation. The foundation type is considered as Winkler-Pasternak foundation type. The first-shear beam theory is used in the kinematics of the beam and the Ritz method is used and in the solution of the problem. In the Ritz method, algebraic polynomials are used with the trivial functions. In the numerical examples, the effects of fibre orientation angles, the volume fraction and foundation parameters on the static deflections of fiber reinforced composite beam are investigated. The numerical results show that fiber orientation angle, volume fraction and foundation parameter have great influence on static behavior of fiber reinforced composites.

Keywords: Fiber Reinforced Composite Material; Static Analysis; Winkler-Pasternak Foundation; Ritz Method

1. Introduction

Fiber reinforced composite (FRC) structures are used in a lot of engineering applications, for example, airplanes, machine, marine, and civil engineering projects. FRC structures mainly preferred in the engineering projects due to their higher strength-weight ratios, more lightweight and ductile properties.

In the literature, many researchers investigated the static, dynamic and stability analyses of FRC structures in last decades. Some investigations about of FRC structures are as follows; Krawczuk et al. [1] studied the vibration of cracked composite beams. Shen [2] presented post-buckling analysis of laminated plate with thermal effects resting on elastic foundation. Sayman [3] investigated elastic-plastic analysis of aluminum metal-matrix laminated plate under thermal effect. Shukla et al. [4] presented thermal postbuckling analysis of laminated plates. Emery et al. [5] analyzed thermoelastic stress analysis of laminated orthotropic plates. Shen [6] presented thermal nonlinear analysis of functionally graded nanocomposite plates reinforced by single-walled carbon nanotubes. Akgöz and Civalek [7,8,9,10] presented mechanical behavior of composite structure resting on foundation.

Kishore et al. [11] investigated nonlinear analysis of magnetostrictive layered plate by using third order shear deformation theory. Sahoo and Singh [12] analyzed static of layered composite plates by using the hyperbolic zigzag theory. Houmat [13] presented nonlinear vibration of laminated composite plates with curvilinear fibers. Khorshid and Farhadi [14] analyzed hydrostatic vibration analysis of a laminated composite rectangular plate partially contacting with a bounded fluid. DeValve and Pitchumani [15] investigated damping vibration analysis of rotating composite beams with embedded carbon nanotubes. Tornabene et al. [16] investigated static and vibration analysis of laminated doubly-curved shells and panels embedded in elastic foundation by using the generalized differential quadrature. Akbaş [17-22] presented free vibration of functionally graded composite beams. Yüksel and Akbaş [23] presented thermal effects of laminated plates by using the Navier method. Draiche et al. [24] presented static analysis of laminated reinforced composite plates based on first-order shear deformation theory by using the Navier method. Jena et al. [25] analysed dynamic behavior of cracked fiber reinforced composite beams. Zenkour et al. [26] investigated torsional dynamics of carbon nanotubes embedded in viscoelastic medium. Waddar et al. [27] investigated buckling and dynamic response of cenosphere reinforced epoxy composite core sandwich beam with sisal fabric/epoxy composite facings under compressive load by experimentally. Akbaş [28-43] investigated nonlinear behavior and forced vibration analysis of composite structures. Also, many researchers investigated mechanical analysis of composite structures resting on foundation [44-60].

The main purpose of this study is to investigate the effects of the fibre orientation angles, the volume fraction and foundation parameters on the static deflections of the FRC beam in detail. In solution of the problem, first shear deformation beam theory and the energy based Ritz method are used. In the numerical results, the effects of fibre orientation angles, the volume fraction and foundation parameters on the static deflections of the FRC beam are investigated.

2. Formulations

Figure 1 shows a simply supported FRC beam resting on Winkler-Pasternak Foundation with with spring constant k_w and k_p, the length L, the height h and width b under a point load (Q) at midpoint of the beam. When the Pasternak foundation spring constant k_p=0, the foundation model reduces to Winkler type.

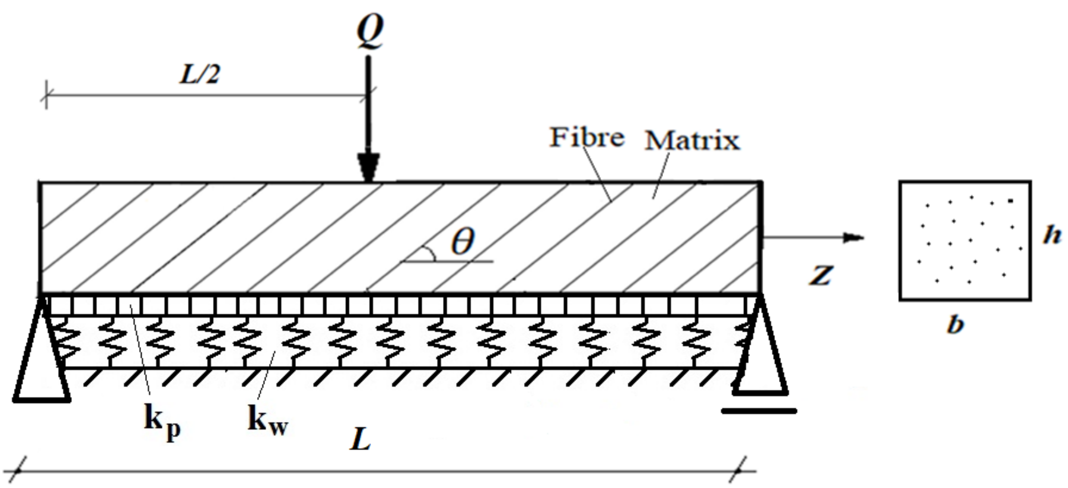

Fig.1. A simply supported FRC beam resting on Winkler-Pasternak Foundation under a point load.

The axial strain (ε_z) and shear strain (γ_{zy}) are given according to the first shear deformation

$$\varepsilon_z = \frac{\partial u}{\partial z} - Y\frac{\partial \emptyset}{\partial z} \tag{1a}$$

$$\gamma_{zy} = \frac{\partial v}{\partial z} - \emptyset \tag{1b}$$

where, u, v and $\emptyset$ are axial displacement, vertical displacement and rotation, respectively. The constitute relation is presented as follows;

$$\begin{Bmatrix} \sigma_z \\ \sigma_{zy} \end{Bmatrix} = \begin{bmatrix} \bar{Q}_{11} & \bar{Q}_{16} \\ \bar{Q}_{16} & \bar{Q}_{66} \end{bmatrix} \begin{Bmatrix} \epsilon_z \\ \gamma_{zy} \end{Bmatrix} \tag{2}$$

where $\bar{Q}_{ij}$ are the transformed components of the reduced constitutive tensor. The transformed components of the reduced constitutive tensor for orthotropic material are as follows:

$$\bar{Q}_{11} = Q_{11}l^4 + 2(Q_{12} + 2Q_{66})l^2n^2 + Q_{22}n^4 \tag{3a}$$

$$\bar{Q}_{12} = (Q_{11} + Q_{22} - 4Q_{66})sin^2cos^2 + Q_{12}(l^4 + n^4) \tag{3b}$$

$$\bar{Q}_{16} = (Q_{11} - Q_{12} - 2Q_{66})nl^3 + (Q_{12} - Q_{22} + 2Q_{66})n^3l \tag{3c}$$

$$\bar{Q}_{22} = Q_{11}n^4 + 2(Q_{12} + 2Q_{66})n^2l^2 + Q_{22}l^4 \tag{3d}$$

$$\bar{Q}_{26} = (Q_{11} - Q_{12} - 2Q_{66})n^3l + (Q_{12} - Q_{22} + 2Q_{66})nl^3 \tag{3e}$$

$$\bar{Q}_{66} = (Q_{11} + Q_{22} - 2Q_{12} - 2Q_{66})n^2l^2 + Q_{66}(n^4 + l^4) \tag{3f}$$

where *l=cos* θ and *n= sin* θ, θ indicates the fiber orientation angle and the expressions of Q_{ij} are as follows;

$$Q_{11} = \frac{E_1}{1-\nu_{12}\nu_{21}}, \quad Q_{22} = \frac{E_2}{1-\nu_{12}\nu_{21}} \tag{4a}$$

$$Q_{12} = \frac{\nu_{12}E_2}{1-\nu_{12}\nu_{21}} = \frac{\nu_{21}E_1}{1-\nu_{12}\nu_{21}} \tag{4b}$$

$$Q_{21} = \frac{\nu_{12}E_2}{1-\nu_{12}\nu_{21}} = \frac{\nu_{21}E_1}{1-\nu_{12}\nu_{21}} \tag{4c}$$

$$Q_{66} = G_{12} \tag{4d}$$

where E_1 is the Young's modulus in the *X* direction, E_2 is the Young's modulus in the *Y* direction, ν_{12} and ν_{21} are Poisson's ratios and G_{12} is the shear modulus in *XY* plane. The gross mechanical properties of the composite materials are calculated by using the following expression (Vinson and Sierakowski [61]):

$$E_1 = E_fV_f + E_m\left(1 - V_f\right), \tag{5a}$$

$$E_2 = E_m\left[\frac{E_f+E_m+(E_f-E_m)V_f}{E_f+E_m-(E_f-E_m)V_f}\right] \tag{5b}$$

$$\nu_{12} = \nu_f\ V_f + \nu_m\left(1 - V_f\right), \tag{5c}$$

$$G_{12} = G_m\left[\frac{G_f+G_m+(G_f-G_m)V_f}{G_f+G_m-(G_f-G_m)V_f}\right] \tag{5d}$$

$$\rho = \rho_fV_f + \rho_m\left(1 - V_f\right), \tag{5e}$$

where *f* indicates the fibre and *m* indicates the matrix. V_f is the volume fraction of fiber. *E*, *G*, *ν* and ρ are the Young's modulus, the shear modulus, Poisson's ratio and mass density, respectively.

The strain energy (U_i), and potential energy of the external loads (U_e) are presented as follows;

$$U_i = \frac{1}{2}\int_0^L \left[A_0\left(\frac{\partial u_0}{\partial z}\right)^2 - 2A_1\frac{\partial u_0}{\partial z}\frac{\partial \emptyset}{\partial z} + A_2\left(\frac{\partial \emptyset}{\partial z}\right)^2\right] dZ + \frac{1}{2}\int_0^L K_s B_0\left[\left(\frac{\partial v_0}{\partial z}\right)^2 - 2\frac{\partial v_0}{\partial z}\emptyset + \emptyset^2\right] dZ + \frac{1}{2}\int_0^L \left(k_w (v_0)^2 + k_p\left(\frac{\partial v_0}{\partial z}\right)^2\right) dZ \tag{6a}$$

$$U_e = -Q(t)\, v\big(z_p, t\big) \tag{6b}$$

where,

$$(A_0, A_1, A_2) = \int_A \overline{Q}_{11}(1, Y, Y^2) dA\,,\ B_0 = \int_A \overline{Q}_{66} dA, \tag{7}$$

The total potential energy of the problem is expressed as follows:

$$\Pi = (U_i - U_e) \tag{8}$$

In the solution of the problem in Ritz method, approximate solution is given as series of *i* terms of the following form:

$$u(z) = \sum_{i=1}^{\infty} \mathrm{a}_i\, \alpha_i(z) \tag{9a}$$

$$v(z) = \sum_{i=1}^{\infty} \mathrm{b}_i\, \beta_i(z) \tag{9b}$$

$$\emptyset(z) = \sum_{i=1}^{\infty} \mathrm{c}_i\, \gamma_i(z) \tag{9c}$$

where a_i, b_i and c_i are the unknown coefficients, $\alpha_i(z)$, $\beta_i(z)$, $\gamma_i(z)$ are the coordinate functions depend on the boundary conditions over the interval [0,L]. The coordinate functions for the simply supported beam are given as algebraic polynomials:

According to the minimum total potential energy principle, unknown coefficients $a_{i,}$, b_i , c_i which correspond to the minimum of the total potential energy (Π) are determined by the conditions:

$$\frac{\partial \Pi}{\partial a_i} = 0\,,\ \frac{\partial \Pi}{\partial b_i} = 0\,,\ \frac{\partial \Pi}{\partial c_i} = 0 \tag{10}$$

Differentiation of *Π* in respect to unknown coefficients produces the following equilibrium equations:

$$[\mathrm{K}]\{\mathrm{q}\} = \{\mathrm{F}\} \tag{11}$$

where $[K]$ and {F} are the stiffness matrix and load vector, respectively. The detail of these expressions are given as follows;

$$[K] = \begin{bmatrix} K_{11} & K_{12} & K_{13} \\ K_{21} & K_{22} & K_{23} \\ K_{31} & K_{32} & K_{33} \end{bmatrix} \tag{12}$$

Where

$$K_{ij}^{11} = \sum_{i=1}^{n}\sum_{j=1}^{n}\int_0^L A_0 \frac{\partial\alpha_i}{\partial z}\frac{\partial\alpha_j}{\partial z} dz \, , K_{ij}^{12} = 0 \, ,$$
$$K_{ij}^{13} = -\sum_{i=1}^{n}\sum_{j=1}^{n}\int_0^L A_1 \frac{\partial\alpha_i}{\partial z}\frac{\partial\gamma_j}{\partial z} dz, K_{ij}^{21} = 0,$$
$$K_{ij}^{22} = \sum_{i=1}^{n}\sum_{j=1}^{n}\int_0^L K_s B_0 \frac{\partial\beta_i}{\partial z}\frac{\partial\beta_j}{\partial z} + \beta_i\beta_j k_w + \frac{\partial\beta_i}{\partial z}\frac{\partial\beta_j}{\partial z} k_p dz,$$
$$K_{ij}^{23} = -\sum_{i=1}^{n}\sum_{j=1}^{n}\int_0^L K_s B_0 \frac{\partial\beta_i}{\partial z}\gamma_j \, dz,$$
$$K_{ij}^{31} = -\sum_{i=1}^{n}\sum_{j=1}^{n}\int_0^L A_1 \frac{\partial\gamma_i}{\partial z}\frac{\partial\alpha_j}{\partial z} dz,$$
$$K_{ij}^{32} = -\sum_{i=1}^{n}\sum_{j=1}^{n}\int_0^L K_s B_0 \gamma_i \frac{\partial\beta_j}{\partial z} dz,$$
$$K_{ij}^{33} = \sum_{i=1}^{n}\sum_{j=1}^{n}\int_0^L A_2 \frac{\partial\gamma_i}{\partial z}\frac{\partial\gamma_j}{\partial z} + \sum_{i=1}^{n}\sum_{j=1}^{n}\int_0^L K_s B_0 \gamma_i\gamma_j \, dz, \tag{13}$$

$$\{\mathrm{F(t)}\} = Q\beta_j \tag{14}$$

The dimensionless quantities can be expressed as

$$\bar{k}_w = \frac{k_w L^4}{E_f I}, \quad \bar{k}_p = \frac{k_p L^2}{E_f I}, \quad \bar{\mathrm{v}} = \frac{\mathrm{v}}{L} \tag{15}$$

$\bar{k}_w$ and $\bar{k}_p$ are the dimensionless Winkler Pasternak parameters, $\bar{\mathrm{v}}$ is lateral dimensionless displacement.

3. Numerical Results

In the numerical study, static displacements of the FRC simply supported beam are presented and discussed. In the numerical examples, the materials of the beams are selected as made of graphite fibre-reinforced polyamide composite and its material parameters are as follows (Krawczuk et al [1]); E_m = 2.756 GPa, E_f = 275.6 GPa, Gm = 1.036 GPa, G_f = 114.8 GPa, ν_m = 0.33, νf = 0.2. The geometry properties of the beam are selected as $b = 0.1$ m, h=0.1 m and L=1.2 m. In the numerical results, number of the series term is taken as 10. The load value is selected as Q_0=1000 kN.

In figure 2, effects of the volume fraction of fiber (v_f) on the lateral static dimensionless displacements of FRC beam at midpoint ($\bar{\mathrm{v}}_m$) are presented with effects of foundation parameter for $\theta = 30$. It is seen from figure 2 that, displacements of the FRC beam decrease with increasing of the volume fraction of fiber and foundation stiffness parameters due to the bending rigidity increases according to Eq. 5. With increasing of foundation stiffness parameters, the difference among the results of v_f decreases considerably. It is seen from figures 2 that Pasternak parameter $\bar{k}_p$ is more effective than Winkler parameter $\bar{k}_w$ on the behavior of the volume fraction of fiber.

In figure 3, effects of the fiber orientation angles (θ) on the lateral static dimensionless displacements of FRC beam at midpoint ($\bar{\mathrm{v}}_m$) are presented with effects of foundation parameter for v_f=0.3. Figure 3 shows that, displacements of the FRC beam increase with increasing of the fiber orientation angles (θ) due to the bending rigidity increases according to

Eq. 3. It is observed from figure 3, Pasternak parameter $\bar{k}_p$ is more effective on the results of fiber orientation angles like the results of the volume fraction of fiber.

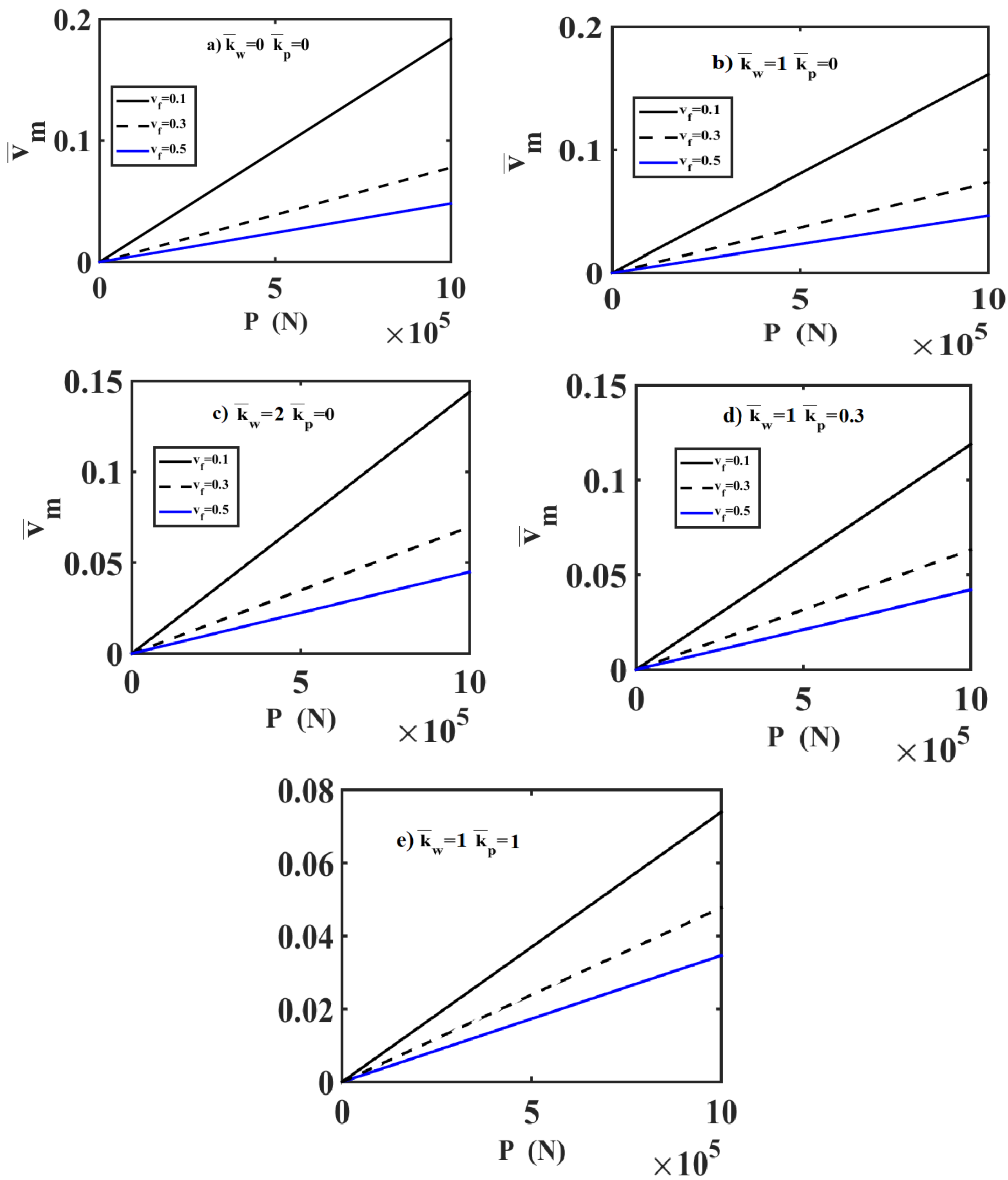

Fig.2. Load – dimensionless lateral displacement (at midpoint) relation for different values of the volume fraction of fiber (v_f) for a) $\bar{k}_w = 0$, $\bar{k}_p = 0$ b) $\bar{k}_w = 1$, $\bar{k}_p = 0$, c) $\bar{k}_w = 2$, $\bar{k}_p = 0$, d) $\bar{k}_w = 1$, $\bar{k}_p = 0.3$, e) $\bar{k}_w = 1$, $\bar{k}_p = 1$

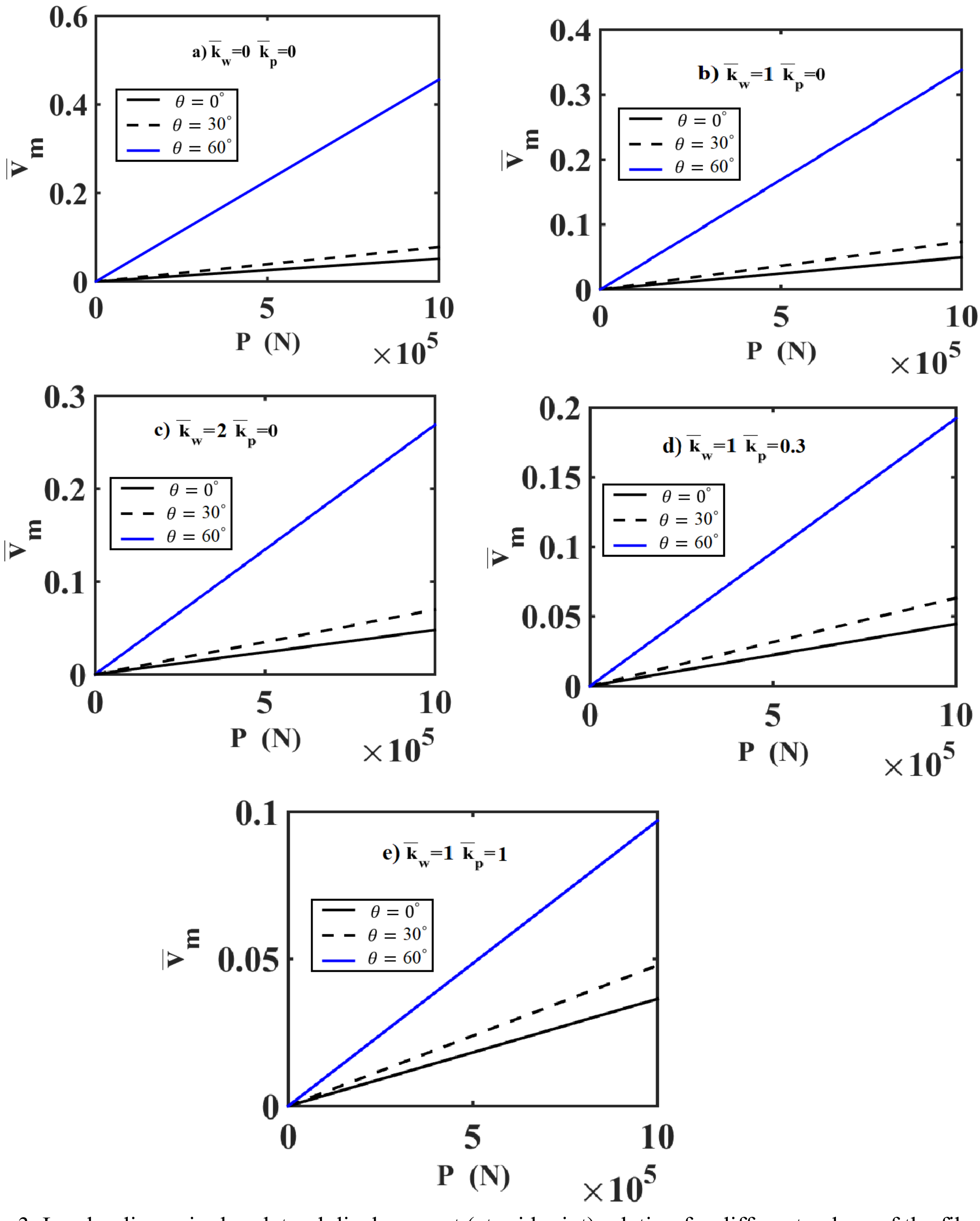

Fig.3. Load – dimensionless lateral displacement (at midpoint) relation for different values of the fiber orientation angles (θ) for a) $\bar{k}_w = 0$, $\bar{k}_p = 0$ b) $\bar{k}_w = 1$, $\bar{k}_p = 0$, c) $\bar{k}_w = 2$, $\bar{k}_p = 0$, d) $\bar{k}_w = 1$, $\bar{k}_p = 0.3$, e) $\bar{k}_w = 1$, $\bar{k}_p = 1$

4. Conclusions

Effects of Winkler-Pasternak foundation parameters and composite material parameters on the static displacements of the FRC simply supported beam are investigated in this paper by using the first shear deformation beam theory. In solution of the problem, the energy based Ritz method is implemented. The presented results show that the displacements of FRC beam change significantly with fiber orientation angle and the volume fraction. The Pasternak parameter is a great influence on behavior of material properties of FRC.

References

[1] Krawczuk, M., Ostachowicz W., Zak, A., Modal analysis of cracked, unidirectional composite beam, *Composites Part B: Engineering*, 28(5-6), 641-650, 1997.

[2] Shen, H.S., Thermal postbuckling behavior of imperfect shear deformable laminated plates with temperature-dependent properties. *Computer Methods in Applied Mechanics and Engineering*, 190(40-41), 5377-5390, 2001.

[3] Sayman, O., Elastic-plastic and residual stresses in symmetric aluminum metal-matrix laminated plates under a linear thermal loading. *Journal of Thermal Stresses*, 26(4), 391-406, 2003.

[4] Shukla, K.K., Huang, J.H., Nath, Y., Thermal postbuckling of laminated composite plates with temperature dependent properties. *Journal of Engineering Mechanics*, 130(7), 818-825, 2004.

[5] Emery, T.R., Dulieu-Barton, J.M., Earl, J.S., Cunningham, P.R. A generalised approach to the calibration of orthotropic materials for thermoelastic stress analysis. *Composites Science and Technology*, 68(3-4), 743-752, 2008.

[6] Shen, H.S., Nonlinear bending of functionally graded carbon nanotube-reinforced composite plates in thermal environments. *Composite Structures*, 91(1), 9-19, 2009.

[7] Akgoz, B., Civalek, O., Nonlinear vibration analysis of laminated plates resting on nonlinear two-parameters elastic foundations. *Steel and Composite Structures*, *11*(5), 403-421, 2011.

[8] Akgöz, B., Civalek, Ö.,Thermo-mechanical buckling behavior of functionally graded microbeams embedded in elastic medium. *International Journal of Engineering Science*, *85*, 90-104, 2014.

[9] Akgöz, B., Civalek, Ö., Modeling and analysis of micro-sized plates resting on elastic medium using the modified couple stress theory. *Meccanica*, *48*(4), 863-873, 2013.

[10] Akgöz, B., Civalek, Ö., Bending analysis of embedded carbon nanotubes resting on an elastic foundation using strain gradient theory. *Acta Astronautica*, *119*, 1-12, 2016.

[11] Kishore, M.H., Singh, B.N., Pandit, M.K., Nonlinear static analysis of smart laminated composite plate. *Aerospace Science and Technology*, 15(3), 224-235, 2011.

[12] Sahoo, R., Singh, B.N., A new inverse hyperbolic zigzag theory for the static analysis of laminated composite and sandwich plates. *Composite structures*, 105, 385-397, 2013.

[13] Houmat, A., Nonlinear free vibration of laminated composite rectangular plates with curvilinear fibers. *Composite Structures*, 106, 211-224, 2013.

[14] Khorshid, K., Farhadi, S., Free vibration analysis of a laminated composite rectangular plate in contact with a bounded fluid. *Composite structures*, 104, 176-186, 2013.

[15] DeValve, C. and Pitchumani, R. (2014), Analysis of vibration damping in a rotating composite beam with embedded carbon nanotubes, *Composite Structures*, 289-296, 2014.

[16] Tornabene, F., Fantuzzi, N., Viola, E. and Reddy, J.N., Winkler–Pasternak foundation effect on the static and dynamic analyses of laminated doubly-curved and degenerate shells and panels, *Composites Part B: Engineering*, **57**, 269-296, 2014.

[17] Akbaş, Ş.D., Static analysis of a functionally graded beam with edge cracks on elastic foundation. In *Proceedings of the 9 th International Fracture Conference, Istanbul, Turkey* (pp. 70-80), 2011.

[18] Akbaş, Ş.D., Free vibration characteristics of edge cracked functionally graded beams by using finite element method. *International Journal of Engineering Trends and Technology*, 4(10), 4590-4597, 2013.
[19] Akbaş, Ş.D., Free vibration of axially functionally graded beams in thermal environment. *International Journal of Engineering & Applied Sciences*, *6*(3), 37-51, 2014.
[20] Akbaş, Ş.D., Free vibration and bending of functionally graded beams resting on elastic foundation. *Research on Engineering Structures and Materials*, 1(1), 2015.
[21] Akbaş, Ş.D., Free Vibration Analysis of Edge Cracked Functionally Graded Beams Resting on Winkler-Pasternak Foundation. *International Journal of Engineering & Applied Sciences*, *7*(3), 1-15, 2015.
[22] Akbaş, Ş.D., Fonksiyonel derecelendirilmiş ortotropik bir kirişin statik ve titreşim davranışlarının incelenmesi. *Balıkesir Üniversitesi Fen Bilimleri Enstitüsü Dergisi*, *20*(1), 69-82, 2018.
[23] Yüksel, Y. Z., Akbaş, Ş. D. (2018). Free vibration analysis of a cross-ply laminated plate in thermal environment. *International Journal of Engineering and Applied Sciences*, *10*(3), 176-189, 2018.
[24] Draiche, K., Bousahla, A.A., Tounsi, A., Alwabli, A. S., Tounsi, A. and Mahmoud, S.R. (2019), "Static analysis of laminated reinforced composite plates using a simple first-order shear deformation theory", *Computers and Concrete* 24(4), 369-378.
[25] Jena, P.C. Parhi, D.R. and Pohit, G. (2016), "Dynamic Study of Composite Cracked Beam by Changing the Angle of Bidirectional Fibres", *Iranian Journal of Science and Technology, Transactions A: Science* 40(1), 27-37.
[26] Zenkour, A. M. (2016), "Torsional Dynamic Response of a Carbon Nanotube Embedded in Visco-Pasternak's Medium", *Mathematical Modelling and Analysis*, **21**(6), 852-868.
[27] Waddar, S., Pitchaimani, J., Doddamani, M., & Barbero, E. (2019), "Buckling and vibration behaviour of syntactic foam core sandwich beam with natural fiber composite facings under axial compressive loads", *Composites Part B: Engineering*, 175, 107133.
[28] Akbaş, Ş.D., Post-buckling analysis of axially functionally graded three-dimensional beams. *International Journal of Applied Mechanics*, *7*(03), 1550047, 2015.
[29] Akbaş, Ş.D., Nonlinear static analysis of functionally graded porous beams under thermal effect. *Coupled Syst. Mech*, *6*(4), 399-415, 2017.
[30] Akbaş, Ş.D., Geometrically nonlinear analysis of functionally graded porous beams. *Wind and Structures*, *27*(1), 59-70, 2018.
[31] Akbaş, Ş.D., Geometrically nonlinear analysis of a laminated composite beam. *Structural Engineering and Mechanics*, *66*(1), 27-36, 2018.
[32] Akbaş, Ş.D., Stability of a non-homogenous porous plate by using generalized differantial quadrature method. *International Journal of Engineering and Applied Sciences*, *9*(2), 147-155, 2017.
[33] Akbaş, Ş.D., Static analysis of a nano plate by using generalized differential quadrature method. *International Journal of Engineering and Applied Sciences*, *8*(2), 30-39, 2016.
[34] Akbaş, Ş.D., Wave propagation analysis of edge cracked beams resting on elastic foundation. *International Journal of Engineering and Applied Sciences*, *6*(1), 40-52, 2014.
[35] Akbaş, Ş.D., Investigation on free and forced vibration of a bi-material composite beam. *Journal of Polytechnic-Politeknik Dergisi*, *21*(1), 65-73, 2018.
[36] Akbaş, Ş.D. Wave propagation of a functionally graded beam in thermal environments. *Steel and Composite Structures*, *19*(6), 1421-1447, 2015.
[37] Akbaş, Ş.D.. (2017). Free vibration of edge cracked functionally graded microscale beams based on the modified couple stress theory. *International Journal of Structural Stability and Dynamics*, *17*(03), 1750033, 2017.

[38] Akbaş, Ş.D., Vibration and static analysis of functionally graded porous plates. *Journal of Applied and Computational Mechanics*, *3*(3), 199-207, 2017.
[39] Akbaş, Ş.D., Thermal post-buckling analysis of a laminated composite beam. *Structural Engineering and Mechanics*, *67*(4), 337-346, 2018.
[40] Akbaş, Ş.D., Geometrically nonlinear analysis of a laminated composite beam. *Structural Engineering and Mechanics*, *66*(1), 27-36, 2018.
[41] Akbaş, Ş.D., Geometrically nonlinear analysis of functionally graded porous beams. *Wind and Structures*, *27*(1), 59-70, 2018.
[42] Akbaş, Ş.D., Hygrothermal post-buckling analysis of laminated composite beams. *International Journal of Applied Mechanics*, *11*(01), 1950009, 2019.
[43] Akbaş, Ş.D., Large deflection analysis of a fiber reinforced composite beam. *Steel and Composite Structures*, *27*(5), 567-576, 2018.
[44] Alsaid-Alwan H.H.S and Avcar, M., Analytical solution of free vibration of FG beam utilizing different types of beam theories: A comparative study, *Computers and Concrete,* 26(3), 285-292, 2020.
[45] Arefi, M., & Civalek, Ö.,Static analysis of functionally graded composite shells on elastic foundations with nonlocal elasticity theory. *Archives of Civil and Mechanical Engineering*, 20(1), 1-17, 2020.
[46] Avcar, M., Free vibration of non-homogeneous beam subjected to axial force resting on Pasternak foundation, *J. Polytechnic*, 19(4), 507-512, 2016.
[47] Avcar, M., Effects of material non-homogeneity and two parameter elastic foundation on fundamental frequency parameters of Timoshenko beams, *Acta Physica Polonica A*, 130(1), 375-378, 2016.
[48] Avcar, M. and Mohammed, W.K.M., Free vibration of functionally graded beams resting on Winkler-Pasternak foundation. *Arabian Journal of Geosciences*, 11(10), 232, 2018.
[49] Bisheh, H. and Civalek, Ö., Vibration of smart laminated carbon nanotube-reinforced composite cylindrical panels on elastic foundations in hygrothermal environments. *Thin-Walled Structures*, 155, 106945, 2020.
[50] Bousahla, A.A., Bourada, F., Mahmoud, S.R., Tounsi, A., Algarni, A., Adda Bedia, E.A., Tounsi, A., Buckling and dynamic behavior of the simply supported CNT-RC beams using an integral-first shear deformation theory, *Computers and Concrete*, 25(2), 155-166, 2020.
[51] Bourada, F., Bousahla, A.A., Tounsi, A., Adda Bedia, E.A., Mahmoud, S.R., Benrahou, K.H., Tounsi, A., "Stability and dynamic analyses of SW-CNT reinforced concrete beam resting on elastic-foundation", *Computers and Concrete*, 25(6), 485-495, 2020.
[52] Civalek, Ö., Avcar, M., Free vibration and buckling analyses of CNT reinforced laminated non-rectangular plates by discrete singular convolution method. *Engineering with Computers*. https://doi.org/10.1007/s00366-020-01168-8, 2020.
[53] Civalek Ö, Acar MH. Discrete singular convolution method for the analysis of Mindlin plates on elastic foundations. *Int J Press Vessel Pip* , 84 (9):527–535, 2007.
[54] Akgöz, B., Civalek, Ö., A size-dependent beam model for stability of axially loaded carbon nanotubes surrounded by Pasternak elastic foundation, Composite Structures, 176, 1028-1038, 2017.
[55] Civalek, Ö., Geometrically non-linear static and dynamic analysis of plates and shells resting on elastic foundation by the method of polynomial differential quadrature (PDQ), Fırat University (in Turkish), Elazığ, Fırat University, 2004.
[56] Civalek, Ö., Kiracioglu, O., Free vibration analysis of Timoshenko beams by DSC method, International Journal for Numerical Methods in Biomedical Engineering, 26(12), 1890-1898, 2010.

[57] Civalek, Ö., Yavas, A., Large deflection static analysis of rectangular plates on two parameter elastic foundations, International Journal of Science and Technology, 1(1), 43-50 , 2006.
[58] Mercan, K., Demir, Ç., Civalek, Ö., Vibration analysis of FG cylindrical shells with power-law index using discrete singular convolution technique, Curved and Layered Structures, 3(1), 82-90, 2016.
[59] Civalek, Ö., Geometrically nonlinear dynamic and static analysis of shallow spherical shell resting on two-parameters elastic foundations, International Journal of Pressure Vessels and Piping, 113, 1-9, 2014.
[60] Civalek, Ö., Finite Element analysis of plates and shells. Elazığ, Fırat University (in Turkish), 1998.
[61] Vinson, J.R. and Sierakowski, R.L., Behaviour of structures composed of composite materials, Kluwer Academic Publishers, ISBN 978-140-2009-04-4, Netherlands, 2002.

International Journal of Engineering & Applied Sciences (IJEAS)
Vol. 12, Issue 3 (2020) 99-110
http://dx.doi.org/10.24107/ijeas.784042
Int J Eng Appl Sci 12(3) (2020) 99-110

Thermal Vibration of Zinc Oxide Nanowires by using Nonlocal Finite Element Method

Hayri Metin Numanoğlu

Giresun University, Civil Engineering Department, Division of Mechanics, 28200, Giresun, Turkey
**E-mail address*: metin_numanoglu@hotmail.com

ORCID numbers of author:
0000-0003-0556-7850

Received date: 22.08.2020
Accepted date: 04.12.2020

Abstract

Zinc oxide nanowires (ZnO NWs) can be used in some NEMS applications due to their remarkable chemical, physical, mechanical and thermal resistance properties. In terms of the suitability of such NEMS organizations, a correct mechanical model and design of ZnO NWs should also be established under different effects. In this study, thermal vibration analyses of elastic beam models of ZnO NWs are examined based on Eringen's nonlocal elasticity theory. The resulting equation of motion is solved with a finite element formulation developed for the atomic size-effect and thermal environment. The vibration frequencies of ZnO NWs with different boundary conditions are calculated under nonlocal parameter and temperature change values and numerical results were discussed.

Keywords: Finite element method, nonlocal elasticity, thermal environment, vibration, Zinc Oxide nanowire.

1. Introduction

It is seen that people use products with stronger physical, chemical, thermal, mechanical, optical, etc. properties. This is possible with the science of nanotechnology that is today's pioneer technology. Nanotechnology is a science that aims to investigate the properties of materials with dimensions from 1 nm to 100 nm and to integrate these materials into classical applications of science and engineering disciplines. It can be stated that nanotechnology, which started its adventure with gave a conference by R. Feynman [1] in 1959, gained a serious importance with the discovery of the carbon nanotube material [2,3]. Additionally, properties of wide range of nanomaterials such as boron nitride nanotube [4], graphene [5] and metallic or molecular nanowires [6-8] are fundamental topics of this discipline. It can be expressed that such nanomaterials show their effect in different applications such as sensor, switch, actuator, bridge, transistor.

The structural-electronic applications containing nanomaterials are generally collected under the name of nanoelectromechanical systems (NEMS). To perform the accurate mechanical analyses of NEMS is essential for NEMS applications to work properly in terms of engineering. To perform mechanical analysis via experimental methods requires high operation costs, professional expert approaches and long processes. Also, it is a well-known fact that the results obtained by experimental methods do not present results in accordance with the classical elasticity theory. These difficulties have been overcome by adapting the mathematical approaches developed in different periods to the classical elasticity theory. The new elasticity theories, namely, higher-order continuum theories, generally include parameters related to the atomic dimensions of nanomaterials. It can be said that nonlocal elasticity theory [9-10], couple stress elasticity theory [11,12], strain gradient elasticity theory [13,14], surface energy elasticity theory [15,16] and doublet mechanics elasticity theory [17] exemplify for higher-order continuum theories.

The nonlocal elasticity theory states that the stress and strain of other regions adjacent to that region must also be taken into consideration in order to calculate the stress and strain in a certain region of the atomic structure. Thus, the uncertainty in the strain energy that goes to infinity due to atomic factors is resolved. In the 1960s, the studies of Eringen et al. enabled the establishment of the nonlocal elasticity theory and the determination of its main principles. It can be stated that approximately 45 years later, analyses of continuous mechanical models of nanoscaled structures started to be handled with the nonlocal elasticity theory [18-20]. Following these, vibration, buckling and bending analyses of nonlocal Euler–Bernoulli nano beams are given [21-23]. Lu et al. studied the nonlocal vibration phase velocities of single and multi-walled carbon nanotubes by using Euler-Bernoulli and Timoshenko beam theories [24]. Numanoğlu examined axial and flexural vibration analyses of different nanowires and nanotubes [25]. Axial and torsional vibration analyses of nonlocal nanorods are also available in the literature [26-32]. Jalaei and Civalek studied the nonlocal elasticity dynamic instability of functionally graded porous beam under magnetic effects resting on viscoelastic foundation by employing Navier's technique and Bolotins's approach [33]. Apart from these, vibration and bending of some nanomaterials are tackled based on the classical theory [34-36]. Civalek presented the finite element formulations of plates and shells [37]. On the other hand, it can be stated that studies on the use of finite element formulation in mechanical analysis of nanostructures with nonlocal elasticity have taken place in the literature [27,28,38-52]. Additionally, the free vibration behavior of a functionally graded beam is researched for Euler-Bernoulli, Timoshenko, Shear and Rayleigh beam theories [53]. Moreover, mechanical analyses of different continuous structures have been performed via novel numerical approaches such as discrete singular convolution and differential quadrature [54-60].

In this article, vibration analyses of nanobeams modeled by using zinc oxide nanowires (ZnO NWs), which has an important area in the applications of nanotechnology science, are carried out with the nonlocal elasticity theory. The temperature effect is considered in the vibration analysis. A nonlocal finite element formulation (NL-FEM) is presented for the solution of equation of motion. Then, the vibration frequencies of simply supported ZnO NWs are calculated via analytical method and NL-FEM and compared. Also, thermal vibration frequency results are presented by using NL-FEM for beam models with boundary condition that is not possible to be solve analytically. In the solution of nonlocal free vibration, the accuracy of the proposed formulation is discussed. Finally, the most general results are summarized.

2. Nonlocal Finite Element Analysis for Thermal Vibration of Nanobeams

The equation of motion of nonlocal thermal vibration of nano scaled beams according to Euler-Bernoulli beam theory can be presented as follows:

$$\left[EI-(e_0a)^2 EA\alpha\Delta T\right]\frac{\partial^4 w}{\partial x^4}+EA\alpha\Delta T\frac{\partial^2 w}{\partial x^2}-f+\rho A\frac{\partial^2 w}{\partial t^2}-(e_0a)^2\rho A\frac{\partial^4 w}{\partial x^2\partial t^2}$$
$$+(e_0a)^2\frac{\partial^2 f}{\partial x^2}=0 \tag{1}$$

where EI is bending rigidity, e_0a is nonlocal parameter and EA is axial rigidity. α defines the thermal expansion coefficient. ΔT is temperature change and w is transverse displacement. On the other hand, ρA explains volume of unit length and f is transverse distributed force.

The solution of Eq. (1) will be performed in this current study by using finite element. The fundamental of this solution based on weighted residual method [49]. According to this, average weighted residue is written as

$$\mathrm{I}=\int_0^l h\left(\left[EI-(e_0a)^2 EA\alpha\Delta T\right]\frac{\partial^4 w}{\partial x^4}+EA\alpha\Delta T\frac{\partial^2 w}{\partial x^2}-f+\rho A\frac{\partial^2 w}{\partial t^2}-(e_0a)^2\rho A\frac{\partial^4 w}{\partial x^2\partial t^2}\right.$$
$$\left.+(e_0a)^2\frac{\partial^2 f}{\partial x^2}=0\right)\mathrm{d}x \tag{2}$$

here, h is weighting function and l is length of finite element. The transverse motion of bending finite element is described as

$$w=\phi\mathbf{w} \tag{3}$$

where ϕ is shape function of beam finite element and $\mathbf{w}$ is displacement vector. Additionally, the first derivation of displacement of bending finite element can be written as

$$\frac{\partial w}{\partial x}=\mathrm{D}^{\mathrm{k}}w=\mathbf{Bw} \tag{4}$$

where $\mathrm{D}^{\mathrm{k}}\phi=\mathbf{B}$ and D^{k} is defined as kinematic operator.

The partial integrations of all terms seen in Eq. (2) can be written as

$$\mathrm{I}_1=\int_0^l EIh\frac{\partial^4 w}{\partial x^4}\mathrm{d}x=EIh\frac{\partial^3 w}{\partial x^3}\bigg|_0^l-EI\frac{\partial h}{\partial x}\frac{\partial^2 w}{\partial x^2}\bigg|_0^l+\int_0^l EI\frac{\partial^2 h}{\partial x^2}\frac{\partial^2 w}{\partial x^2}\mathrm{d}x,$$
$$\mathrm{I}_2=\int_0^l (e_0a)^2 EA\alpha\Delta Th\frac{\partial^4 w}{\partial x^4}\mathrm{d}x=(e_0a)^2 EA\alpha\Delta Th\frac{\partial^3 w}{\partial x^3}\bigg|_0^l-(e_0a)^2 EA\alpha\Delta T\frac{\partial h}{\partial x}\frac{\partial^2 w}{\partial x^2}\bigg|_0^l$$
$$+\int_0^l (e_0a)^2 EA\alpha\Delta T\frac{\partial^2 h}{\partial x^2}\frac{\partial^2 w}{\partial x^2}\mathrm{d}x,$$
$$\mathrm{I}_3=\int_0^l EA\alpha\Delta Th\frac{\partial^2 w}{\partial x^2}\mathrm{d}x=EA\alpha\Delta Th\frac{\partial w}{\partial x}\bigg|_0^l-\int_0^l EA\alpha\Delta T\frac{\partial h}{\partial x}\frac{\partial w}{\partial x}\mathrm{d}x,$$

$$\mathrm{I}_4 = \int_0^l hf\,\mathrm{d}x,\ \mathrm{I}_5 = \int_0^l \rho A h \frac{\partial^2 w}{\partial t^2}\mathrm{d}x,$$

$$\mathrm{I}_6 = \int_0^l (e_0 a)^2 \rho A h \frac{\partial^4 w}{\partial x^2 \partial t^2}\mathrm{d}x = (e_0 a)^2 \rho A h \frac{\partial^3 w}{\partial x \partial t^2}\bigg|_0^l + \int_0^l (e_0 a)^2 \rho A \frac{\partial h}{\partial x}\frac{\partial^3 w}{\partial x \partial t^2}\mathrm{d}x,$$

$$\mathrm{I}_7 = \int_0^l (e_0 a)^2 h \frac{\partial^2 f}{\partial x^2}\mathrm{d}x = (e_0 a)^2 h \frac{\partial f}{\partial x}\bigg|_0^l - \int_0^l (e_0 a)^2 \frac{\partial h}{\partial x}\frac{\partial f}{\partial x}\mathrm{d}x, \tag{5}$$

If above equations are substituted into Eq. (2) and weighted residual is evanished, the weak formulation is attained as follows

$$\int_0^l EI \frac{\partial^2 h}{\partial x^2}\frac{\partial^2 w}{\partial x^2}\mathrm{d}x - \int_0^l (e_0 a)^2 EA\alpha\Delta T \frac{\partial^2 h}{\partial x^2}\frac{\partial^2 w}{\partial x^2}\mathrm{d}x - \int_0^l EA\alpha\Delta T \frac{\partial h}{\partial x}\frac{\partial w}{\partial x}\mathrm{d}x$$
$$- \int_0^l hf\,\mathrm{d}x + \int_0^l \rho A h \frac{\partial^2 w}{\partial t^2}\mathrm{d}x + \int_0^l (e_0 a)^2 \rho A \frac{\partial h}{\partial x}\frac{\partial^3 w}{\partial x \partial t^2} - \int_0^l (e_0 a)^2 \frac{\partial h}{\partial x}\frac{\partial f}{\partial x}\mathrm{d}x = 0 \tag{6}$$

To rearrange Eq. (6), following expressions can be used:

$$h = \phi^{\mathrm{T}},\quad \frac{\partial h}{\partial x} = \left(\phi^{\mathrm{T}}\right)' = \mathbf{B}^{\mathrm{T}},\quad \frac{\partial^2 w}{\partial x^2} = \mathbf{B}'\mathbf{w},\quad \frac{\partial^2 w}{\partial t^2} = \phi\ddot{\mathbf{w}} \tag{7}$$

Substituting of Eq. (7) into Eq. (6) yields following equation

$$\int_0^l EI\left(\mathbf{B}'^{\mathrm{T}}\mathbf{B}'\right)\mathbf{w}\mathrm{d}x - \int_0^l (e_0 a)^2 EA\alpha\Delta T\left(\mathbf{B}'^{\mathrm{T}}\mathbf{B}'\right)\mathbf{w}\mathrm{d}x - \int_0^l EA\alpha\Delta T\left(\mathbf{B}^{\mathrm{T}}\mathbf{B}\right)\mathbf{w}\mathrm{d}x - \int_0^l \phi^{\mathrm{T}} f\mathrm{d}x$$
$$+ \int_0^l \rho A\left(\phi^{\mathrm{T}}\phi\right)\ddot{\mathbf{w}}\mathrm{d}x + \int_0^l (e_0 a)^2 \rho A\left(\mathbf{B}^{\mathrm{T}}\mathbf{B}\right)\ddot{\mathbf{w}}\mathrm{d}x - \int_0^l (e_0 a)^2 \mathbf{B}^{\mathrm{T}} f'\mathrm{d}x = 0 \tag{8}$$

this equation can be written as follows in the matrix form:

$$\left(K - K_{T,c} - K_{T,nl}\right)\mathbf{w} + \left(M_c + M_{nl}\right)\ddot{\mathbf{w}} = \mathbf{f}_c + \mathbf{f}_{nl} \tag{9}$$

In here,

$$K = \int_0^l EI\left(\mathbf{B}'^{\mathrm{T}}\mathbf{B}'\right)\mathrm{d}x = \int_0^l EI\begin{Bmatrix}\phi_1'' \\ \phi_2'' \\ \phi_3'' \\ \phi_4''\end{Bmatrix}\begin{bmatrix}\phi_1'' & \phi_2'' & \phi_3'' & \phi_4''\end{bmatrix}\mathrm{d}x = \frac{EI}{l^3}\begin{bmatrix}12 & 6l & -12 & 6l \\ 6l & 4l^2 & -6l & 2l^2 \\ -12 & -6l & 12 & -6l \\ 6l & 2l^2 & -6l & 4l^2\end{bmatrix} \tag{10}$$

$$K_{T,c}=\int_0^l EA\alpha\Delta T\left(\mathbf{B}^{\mathrm{T}}\mathbf{B}\right)\mathrm{d}x=\int_0^l EA\alpha\Delta T\begin{Bmatrix}\phi_1'\\ \phi_2'\\ \phi_3'\\ \phi_4'\end{Bmatrix}\begin{bmatrix}\phi_1' & \phi_2' & \phi_3' & \phi_4'\end{bmatrix}\mathrm{d}x$$

$$=\frac{EA\alpha\Delta T}{30L}\begin{bmatrix}36 & 3l & -36 & 3l\\ 3l & 4l^2 & -3l & -l^2\\ -36 & -3l & 36 & -3l\\ 3l & -l^2 & -3l & 4l^2\end{bmatrix} \tag{11}$$

$$K_{T,nl}=\int_0^l (e_0a)^2 EA\alpha\Delta T\left(\mathbf{B}'^{\mathrm{T}}\mathbf{B}'\right)\mathrm{d}x=\int_0^l (e_0a)^2 EA\alpha_L\Delta T\begin{Bmatrix}\phi_1''\\ \phi_2''\\ \phi_3''\\ \phi_4''\end{Bmatrix}\begin{bmatrix}\phi_1'' & \phi_2'' & \phi_3'' & \phi_4''\end{bmatrix}\mathrm{d}x$$

$$=\frac{(e_0a)^2 EA\alpha_L\Delta T}{l^3}\begin{bmatrix}12 & 6l & -12 & 6l\\ 6L & 4l^2 & -6l & 2l^2\\ -12 & -6l & 12 & -6l\\ 6L & 2l^2 & -6l & 4l^2\end{bmatrix} \tag{12}$$

$$M_c=\int_0^l \rho A\left(\phi^{\mathrm{T}}\phi\right)\mathrm{d}x=\int_0^l \rho A\begin{Bmatrix}\phi_1\\ \phi_2\\ \phi_3\\ \phi_4\end{Bmatrix}\begin{bmatrix}\phi_1 & \phi_2 & \phi_3 & \phi_4\end{bmatrix}\mathrm{d}x=\frac{\rho Al}{420}\begin{bmatrix}156l & 22l^2 & 54l & -13l^2\\ 22l^2 & 4l^3 & 13l^3 & -3l^3\\ 54l & 13l^2 & 156l & -22l^2\\ -13l & -3l^3 & -22l^2 & 4l^3\end{bmatrix} \tag{13}$$

$$M_{nl}=\int_0^l (e_0a)^2\rho A\left(\mathbf{B}^{\mathrm{T}}\mathbf{B}\right)\mathrm{d}x=\int_0^l (e_0a)^2\rho A\begin{Bmatrix}\phi_1'\\ \phi_2'\\ \phi_3'\\ \phi_4'\end{Bmatrix}\begin{bmatrix}\phi_1' & \phi_2' & \phi_3' & \phi_4'\end{bmatrix}\mathrm{d}x$$

$$=\frac{(e_0a)^2\rho A}{30l}\begin{bmatrix}36 & 3l & -36 & 3l\\ 3l & 4l^2 & -3l & -l^2\\ -36 & -3l & 36 & -3l\\ 3l & -l^2 & -3l & 4l^2\end{bmatrix} \tag{14}$$

$$\mathbf{f}_c=\int_0^l f\phi^{\mathrm{T}}\mathrm{d}x=\int_0^l f\begin{Bmatrix}\phi_1\\ \phi_2\\ \phi_3\\ \phi_4\end{Bmatrix}\mathrm{d}x=\frac{l}{12}f\begin{Bmatrix}6\\ l\\ 6\\ -l\end{Bmatrix} \tag{15}$$

$$\mathbf{f}_{nl} = \int_0^l (e_0 a)^2 f' \mathbf{B}^{\mathrm{T}} \mathrm{d}x = \int_0^l (e_0 a)^2 f' \begin{Bmatrix} \phi_1' \\ \phi_2' \\ \phi_3' \\ \phi_4' \end{Bmatrix} \mathrm{d}x = (e_0 a)^2 f' \begin{Bmatrix} -1 \\ 0 \\ 1 \\ 0 \end{Bmatrix} \tag{16}$$

where K is bending stiffness matrix. $K_{T,c}$ and $K_{T,nl}$ state the local and nonlocal negative stiffness matrices originating from temperature change, respectively. On the other hand, M_c and M_{nl} are local and nonlocal mass matrices, respectively. $\mathbf{f}_c$ and $\mathbf{f}_{nl}$ express local and nonlocal external force vectors, respectively.

If the $f = 0$ is taken for free vibration and $w(x,t) = W(x)\sin(\omega t - \alpha)$ expression is utilized into Eq. (9), the eigenvalue formulation of finite element analysis is obtained as follows:

$$\det\left(\sum[K] - \omega^2 \sum[M]\right) = 0 \tag{17}$$

where $\sum[K]$ and $\sum[M]$ are total stiffness and mass matrices. ω is natural frequency of nanobeam.

Also, the frequency equation of simply supported beams can be solved analytically. According to this, the series expansion as follows, ensures geometric and mechanical boundary conditions of simply supported beams:

$$w(x,t) = \sum_{n=1}^{\infty} W_n \left(\frac{n\pi x}{L}\right) \sin(\omega t - \alpha) \tag{18}$$

where W_n is unknown series coefficient, n is mode number, L is length of nanobeam. ω explains the natural frequency of nanobeam. Additionally, t is time and α is phase angle. Using Eq. (18) into Eq. (1), the following expression can be obtained

$$m_1 \left(\frac{n\pi}{L}\right)^4 + m_2 \left(\frac{n\pi}{L}\right)^2 + m_3 = 0 \tag{19}$$

Where

$$m_1 = EI - (e_0 a)^2 EA\alpha\Delta T, \quad m_2 = -EA\alpha\Delta T - \omega^2 (e_0 a)^2 \rho A, \quad m_3 = -\omega^2 \rho A \tag{20}$$

Substituting of Eq. (20) into Eq. (19) yields the natural frequency equation of simply supported nano beams for nonlocal parameter and temperature change:

$$\omega^2 = \frac{\left[EI - (e_0 a)^2 EA\alpha\Delta T\right]\left(\frac{n\pi}{L}\right)^4 - EA\alpha\Delta T\left(\frac{n\pi}{L}\right)^2}{\rho A\left[(e_0 a)^2 \left(\frac{n\pi}{L}\right)^2 + 1\right]} \tag{21}$$

3. Numerical Examples

In this section, vibration frequencies are calculated for thermal vibration analysis of ZnO NWs. The numerical results are given for simply supported (S-S), cantilever (C-F), propped cantilever (C-S) and clamped supported (C-C) boundary conditions. In order to include the nano scale effect in the analysis, nonlocal elasticity theory is considered. Mechanical properties are taken as follows in the thermal vibration analysis: modulus of elasticity $E = 58\,\text{GPa}$ [61], unit volume mass $\rho = 5600\,\text{kg/m}^3$ [62] and thermal expansion coefficient $\alpha = 2.9\times10^{-6}\,\text{K}^{-1}$ [63]. Additionally, the geometric features are chosen as follows: beam length $L = 20\,\text{nm}$ and circular cross-section diameter $d = 2\,\text{nm}$. On the other hand, 20 finite elements are used for nonlocal finite element analyses.

In Table 1, the first three mode vibration frequencies of simply supported beams modeled with ZnO NWs are calculated and compared with analytical and finite elements for different nondimensional nonlocal parameter values. In addition, the frequencies of the beams not under temperature change were compared with frequencies of the beams under temperature change. First of all, nonlocal expression is a parameter that reduces classical vibration frequencies. By the increase of this value reveals, the frequencies of nanoscaled beams more decrease. Also, temperature change decreases the frequencies of ZnO NWs. In the case that the nonlocal parameter is higher, the temperature factor is more influential. On the other hand, it is seen that the values obtained by the finite element method are very close to the analytically calculated frequencies. In general, while the increase in the mode number raises the difference between calculated values by using the analytical method and NL-FEM, the increase of nonlocal parameter decreases this difference.

In Table 2, the first three mode frequencies of ZnO NWs are tabulated for three different boundary conditions and temperature change. Analytical vibration analysis for boundary conditions except S-S is not possible in case of nonlocal elasticity. Also, when it is considered that the temperature parameter is included in the analysis, an alternative to the analytical method has to be used and therefore the analyses are given only with the finite element formulation. When the stiffness states between the boundary conditions are compared, it can be said that the results obtained are reasonable. The frequencies of the clamped supported beams are the highest, while the frequencies of the cantilever beams are the lowest. Additionally, the boundary condition in which the nonlocal parameter has the highest effect is C-C.

Table 1. Comparison of the first three modes flexural frequencies (GHz) of simply supported Zinc Oxide nanowires.

Nonlocal parameter	Mode Number	$\Delta T = 0\,\text{K}$		$\Delta T = 300\,\text{K}$	
		Analytical	NL-FEM	Analytical	NL-FEM
$e_0a/L = 0$	1	6.3190	6.3190	5.8565	5.8565
	2	25.2761	25.2763	24.8265	24.8266
	3	56.8712	56.8731	56.4238	56.4258
$e_0a/L = 0.15$	1	5.7161	5.7161	5.2002	5.2002
	2	18.3941	18.3942	17.7712	17.7713
	3	32.8423	32.8434	32.0614	32.0625
$e_0a/L = 0.35$	1	4.2516	4.2516	3.5276	3.5276
	2	10.4628	10.4629	9.3244	9.3244
	3	16.4991	16.4997	14.8841	14.8846

Table 2. The first three modes flexural frequencies (GHz) of Zinc Oxide nanowires with different boundary conditions under temperature change.

Nonlocal parameter	Mode Number	Boundary Conditions ($\Delta T = 300\ \mathrm{K}$)		
		C-F	C-S	C-C
$e_0 a/L = 0$	1	1.5191	9.5326	14.0772
	2	13.4342	31.6055	39.1525
	3	38.9400	66.3446	77.0480
$e_0 a/L = 0.15$	1	1.3875	8.3462	12.2447
	2	10.0411	22.1828	26.9237
	3	23.5060	37.0263	42.2733
$e_0 a/L = 0.35$	1	0.9311	5.5268	8.0226
	2	5.6495	11.5262	13.7018
	3	11.6736	17.1731	19.6303

4. Conclusions

In this study, a vibration analysis is performed for elastic beam models of ZnO NWs based on the nonlocal elasticity theory. It is also thought that the beams are under the influence of temperature change. Finite element formulation is used to solve the equation of motion. With this formulation, frequencies of different vibration modes of ZnO NW beams with different boundary conditions are calculated under nondimensional nonlocal parameter and temperature change values and the results are discussed.

In general, it is understood that the atomic scale effect and ambient temperature are definitely factors to be taken into account in the dynamic analysis of continuous models of nanoscale structures. In addition, it is concluded that the use of finite element formulation based on the size effect is an important way for the cases where dynamic analysis cannot be performed by analytical methods. It is thought that these results will guide the proper and optimum structural designs of NEMS using ZnO NWs.

References

[1] Feynman, R.P., There's plenty of room at the bottom. *Engineering and Science*, 23, 22-36, 1960.

[2] Iijima, S., Helical microtubules of graphitic carbon. *Nature*, 354, 56-58, 1991.

[3] Iijima, S., Ichihashi, T., Single-shell carbon nanotubes of 1-nm diameter. *Nature*, 363, 603-605, 1993.

[4] Chopra, N.G., Zettl, A., Measurement of the elastic modulus of a multi-wall boron nitride nanotube. *Solid State Communications*, 105, 297-300, 1997.

[5] Zhu, Y., Murali, S., Cai, W., Li, Suk, J.W., Potts, J.R., Ruoff, R.S. Graphene and Graphene Oxide: Synthesis, Properties, and Applications, *Advanced Materials*, 22, 2010.

[6] Chen, K.I., Li, B.R., Chen, Y.T., Silicon nanowire field-effect transistor-based biosensors for biomedical diagnosis and cellular recording investigation. *Nano Today*, 6, 131-154, 2011.

[7] Liu, Y.Y., Wang, X.Y., Cao, Y., Chen, X.D., Xie, S.F., Zheng, X.J., Zeng, H.D., A flexible blue light-emitting diode based on ZnO nanowire/polyaniline heterojunctions. *Journal of Nanomaterials*, 870254, 2013.

[8] Zhang, P., Wyman, I., Hu, J., Lin, S., Zhong, Z., Tu, Y., Huang, Z., Wei, Y., Silver nanowires: Synthesis Technologies, growth mechanism and multifunctional applications, *Materials Science and Engineering B*, 223, 1–23, 2017.

[9] Eringen, A.C., Edelen, D.G.B., On nonlocal elasticity. *International Journal of Engineering Science*, 10, 233-248, 1972.

[10] Eringen, A.C., On differential equations of non local elasticity and solutions of screw dislocation and surface waves. *Journal of Applied Physics*, 54, 4703, 1983.

[11] Toupin, R.A., Elastic materials with couple-stresses. *Archive for Rational Mechanics and Analysis*, 11, 385-414. 1962.

[12] Koiter, W.T., Couple stresses in the theory of elasticity. *I & II. Philosophical Transactions of the Royal Society of London B*, 67, 17-44, 1964.

[13] Yang, F., Chong, A.C.M., Lam, D.C.C., Tong, P., Couple stress based strain gradient theory for elasticity. *International Journal of Solids and Structures*, 39, 2731-2743, 2002.

[14] Akgöz, B., Civalek, Ö., A size-dependent beam model for stability of axially loaded carbon nanotubes surrounded by Pasternak elastic foundation. *Composite Structures*, 176, 1028-1038, 2017.

[15] Gurtin, M.E., Murdoch, A.I., A continuum theory of elastic material surfaces. *Archive for Rational Mechanics and Analysis*, 57, 291-323, 1975.

[16] Gurtin, M.E., Murdoch, A.I., Surface stress in solids. *International Journal of Solids and Structures*, 14, 431-440. 1978.

[17] Granik, V.T., Ferrari, J.W., Microstructural mechanics of granular media. *Mechanics of Materials*, 15.301-322, 1993.

[18] Sudak, L.J., Column buckling of multiwalled carbon nanotubes using nonlocal continuum mechanics. Journal of Applied Physics, 94, 7281-7287, 2003.

[19] Wang, Q., Liew, K.M., Application of nonlocal continuum mechanics to static analysis of micro- and nano-structures. *Physics Letters A*, 363, 236-242, 2007.

[20] Wang, Q., Varadan, V.K., Vibration of carbon nanotubes studied using nonlocal continuum mechanics. *Smart Materials and Structures*, 15, 659, 2006.

[21] Reddy, J.N., Nonlocal theories for bending, buckling and vibration of beams. *International Journal of Engineering Science*, 45, 288-307, 2007.

[22] Reddy, J.N., Pang, S.D., Nonlocal continuum theories of beams for the analysis of carbon nanotubes. *Journal of Applied Physics*, 103, 023511, 2008.

[23] Ghannadpour, S.A.M., Mohammadi, B., Fazilati, J., Bending, buckling and vibration problems of nonlocal Euler beams using Ritz method. *Composite Structures*, 96, 584-589, 2013.

[24] Lu, P., Lee, H.P., Lu, C., Zhang, P.Q., Application of nonlocal beam models for carbon nanotubes. *International Journal of Solids and Structures*, 44, 5289-5300, 2007.

[25] Numanoğlu, H.M., Vibration analysis of beam and rod models of nanostructures based on nonlocal elasticity theory (In Turkish). BSc. Thesis, Akdeniz University, Antalya, 2017.

[26] Aydogdu, M., Axial vibration of the nanorods with the nonlocal continuum rod model. *Physica E: Low-dimensional Systems and Nanostructures*, 41, 861-864, 2009.

[27] Demir, Ç., Civalek, Ö., Torsional and longitudinal frequency and wave response of microtubules based on the nonlocal continuum and nonlocal discrete models. *Applied Mathematical Modelling*, 37, 9355-9367, 2013.

[28] Lim, C.W., Islam, M.Z., Zhang, G., A nonlocal finite element method for torsional statics and dynamics of circular nanostructures. *International Journal of Mechanical Sciences*, 94-95, 232-243, 2015.

[29] Li, X.-F., Shen, Z.B., Lee, K.Y., Axial wave propagation and vibration of nonlocal nanorods with radial deformation and inertia. *ZAMM Journal of Applied Mathematics and Mechanics: Zeitschrift für Angewandte Mathematik und Mechanik*, 97, 602-616, 2017.

[30] Yayli, M.Ö., On the torsional vibrations of restrained nanotubes embedded in an elastic medium. *Journal of the Brazilian Society of Mechanical Sciences and Engineering*, 40, 419, 2018.

[31] Numanoğlu, H.M., Akgöz, B., Civalek, Ö., On dynamic analysis of nanorods. *International Journal of Engineering Science*, 130, 33-50, 2018.

[32] Karlicic, D.Z., Ayed, S., Flaieh, E., Nonlocal axial vibration of the multiple Bishop nanorod system. *Mathematics and Mechanics of Solids*, 24, 1668-1691, 2018.

[33] Jalaei, M., Civalek, Ö., On dynamic instability of magnetically embedded viscoelastic porous FG nanobeam. *International Journal of Engineering Science*, 143, 14-32, 2019.

[34] Numanoğlu, H.M., Mercan, K., Civalek, Ö., Frequency and mode shapes of Au nanowires using the continuous beam models. *International Journal of Engineering and Applied Sciences*, 9, 55-61, 2017.

[35] Uzun, B., Civalek, Ö., Carbon nanotube beam model and free vibration analysis. *International Journal of Engineering & Applied Sciences*, 10, 1-4, 2018.

[36] Numanoğlu, H.M., Civalek, Ö., Elastic beam model and bending analysis of silver nanowires. *International Journal of Engineering and Applied Sciences*, 10, 13-20, 2018.

[37] Civalek, Ö., Finite Element analysis of plates and shells. Fırat University, Elazığ, 1998.

[38] Adhikari, S., Murmu, T., McCarthy, M.A., Dynamic finite element analysis of axially vibrating nonlocal rods. *Finite Elements in Analysis and Design*, 630, 42-50, 2013.

[39] Adhikari, S., Murmu, T., McCarthy, M.A., Frequency domain analysis of Nonlocal rods embedded in an elastic medium. *Physica E: Low-dimensional Systems and Nanostructures*, 59, 33-40, 2014.

[40] Eltaher, M.A., Alshorbagy, A.E., Mahmoud, F.F., Vibration analysis of Euler–Bernoulli nanobeams by using finite element method. *Applied Mathematical Modelling*, 37, 4787-4797, 2013.

[41] Pradhan, S.C., Mandal, U., Finite element analysis of CNTs based on nonlocal elasticity and Timoshenko beam theory including thermal effect. *Physica E: Low-dimensional Systems and Nanostructures*, 53, 223-232, 2013

[42] Civalek, Ö., Demir, C., A simple mathematical model of microtubules surrounded by an elastic matrix by nonlocal finite element method. *Applied Mathematics and Computation*, 289, 335-352, 2016.

[43] Demir, Ç., Civalek, Ö., A new nonlocal FEM via Hermitian cubic shape functions for thermal vibration of nano beams surrounded by an elastic matrix. Composite Structures, 168, 872-884, 2017.

[44] Işik Ç., Mercan K., Numanoğlu H.M., Civalek Ö., Bending response of nanobeams resting on elastic foundation. *Journal of Applied and Computational Mechanics*, 4, 105-114, 2017.

[45] Uzun B., Numanoğlu H.M., Civalek Ö., Free vibration analysis of BNNT with different cross-sections via nonlocal FEM. *Journal of Computational Applied Mechanics*, 49, 252-260, 2018.

[46] Numanoğlu H.M., Uzun, B., Civalek, Ö., Derivation of nonlocal finite element formulation for nano beams. *International Journal of Engineering and Applied Sciences*, 10, 131-139, 2018.

[47] Numanoğlu H.M., Civalek Ö., On the dynamics of small-sized structures. *International Journal of Engineering Science*, 145, 103164, 2019.

[48] Numanoğlu H.M., Civalek Ö., On the torsional vibration of nanorods surrounded by elastic matrix via nonlocal FEM. *International Journal of Mechanical Sciences*, 161-162, 105076, 2019.

[49] Numanoğlu, H.M., Dynamic analysis of nano continuous and discrete structures based on nonlocal finite element formulation (NL-FEM) (In Turkish). MSc. Thesis, Akdeniz University, Antalya, 2019.

[50] Civalek, Ö., Numanoğlu H.M., Nonlocal finite element analysis for axial vibration of embedded Love–Bishop nanorods. *International Journal of Mechanical Sciences*, 188, 105939, 2020.

[51] Uzun, B., Civalek, O., Nonlocal FEM formulation for vibration analysis of nanowires on elastic matrix with different materials. *Mathematical and Computational Applications*. 24, 38, 2019.

[52] Civalek, O., Uzun, B., Yaylı, M.O., Akgöz, B., Size-dependent transverse and longitudinal vibrations of embedded carbon and silica carbide nanotubes by nonlocal finite element method. *European Physical Journal Plus*, 135, 381, 2020.

[53] AlSaid-Alwan, H.H.S., Avcar, M., Analytical solution of free vibration of FG beam utilizing different types of beam theories: A comparative study. *Computers and Concrete*, 26, 285-292, 2020.

[54] Civalek, Ö., Kiracioglu, O., Free vibration analysis of Timoshenko beams by DSC method. *International Journal for Numerical Methods in Biomedical Engineering*, 26, 1890-1898, 2010.

[55] Civalek, O., Yavas, A., Large deflection static analysis of rectangular plates on two parameter elastic foundations. *International Journal of Science and Technology*, 1, 43-50, 2006.

[56] Civalek, Ö., Geometrically non-linear static and dynamic analysis of plates and shells resting on elastic foundation by the method of polynomial differential quadrature (PDQ) (In Turkish). PhD Thesis, Fırat University, Elazığ, 2004.

[57] Mercan, K., Demir, Ç., Civalek, Ö., Vibration analysis of FG cylindrical shells with power-law index using discrete singular convolution technique. *Curved and Layered Structures* 3, 82-90, 2016.

[58] Civalek, Ö., Geometrically nonlinear dynamic and static analysis of shallow spherical shell resting on two-parameters elastic foundations. *International Journal of Pressure Vessels and Piping*, 113, 1-9, 2014.

[59] Gurses, M., Akgoz, B., Civalek, O., Mathematical modeling of vibration problem of nano-sized annular sector plates using the nonlocal continuum theory via eight-node discrete singular convolution transformation. *Applied Mathematics and Computation*, 219, 3226-3240, 2012.

[60] Civalek, Ö., Avcar, M., Free vibration and buckling analyses of CNT reinforced laminated non-rectangular plates by discrete singular convolution method. *Engineering with Computers*, 2020.

[61] Huang, Y., Bai, X., Zhang, Y., In situ mechanical properties of individual ZnO nanowires and the mass measurement of nanoparticles. *Journal of Physics: Condensed Matter*, 18, L179, 2006.

[62] Zinc Oxide Nanowires. (05.08.2020) https://www.americanelements.com/zinc-oxide-nanowires-1314-13-2. 2019.

[63] Shrama, S.K, Saurakhiya, N., Barthwal, S., Kumar, R., Sharma, A., Tuning of structural, optical, and magnetic properties of ultrathin and thin ZnO nanowire arrays for nano device applications. *Nanoscale Research Letters*, 9, 122, 2014.

International Journal of Engineering & Applied Sciences (IJEAS)
Vol. 12, Issue 3 (2020) 111-124
http://dx.doi.org/10.24107/ijeas.809300
Int J Eng Appl Sci 12(3) (2020) 111-124

A Practical Jointed Approach to Thermal Stress Analysis of FGM Disc

*Ayşegül Özgür [a], Kutay Aydın [b], Ibrahim Keles [c]**

[a] Amasya University, Graduate School of Natural and Applied Sciences, Department of Mechanical Engineering, Amasya 05100, Turkey
[a] Amasya University, Faculty of Technology, Department of Mechanical Engineering, Amasya 05100, Turkey
[b] Samsun University, Faculty of Engineering, Department of Mechanical Engineering, Samsun 55080, Turkey
**E-mail address*: aysegulnimet@hotmail.com [a], kutay.aydin@amasya.edu.tr [b], ibrahim.keles@samsun.edu.tr [c]

ORCID numbers of author:
0000-0001-5024-3180[a], 0000-0003-3614-4877[b], 0000-0001-8252-2635[c]

Received date: 12.10.2020
Accepted date: 06.12.2020

Abstract

In this study, a numerical approach has been introduced in the elastic stress solutions of hollow disks made of functionally graded materials (FGM) that are exposed to linearly increasing temperature dispersion. The modulus of elasticity and the coefficient of thermal expansion of the FGM disk is assumed to vary in radial direction in different forms, and it is further assumed that the Poisson's ratio is constant. It causes the differential equation that manages the behaviour of the object under different material properties and boundary conditions to be a variable coefficient equation. Except for some simple grade materials and boundary conditions, it is hardly possible to produce an analytical solution of such equations. In this case, the solution of the problems can only be found with numerical approaches. Complementary Functions Method (CFM) was used to solve the problem. Different material models were used from the written works and corresponding radial, tangential and equivalent stresses and radial displacements were calculated. Simple, effective and well-structured solution steps can be easily implemented for disks.

Keywords: Functionally Graded Materials, Complementary Functions Method, Hollow Disc, Thermal Stress Analysis.

1. Introduction

The issue of the effect of variable thickness FGM cylindrical materials and high temperatures on these structures has become increasingly popular. Applications of cylindrical FGM structures include aerospace, nuclear power plants, aero-marine and chemical plants where the metals and metal alloys used exhibit elastic behavior. FGMs are variegated materials with continuous fluctuation of elastic and thermal properties throughout the material. Constituent materials having various properties are formed by methodically changing the bulk portion of the materials. The materials used in FGM applications are heat resistant, corrosion durable, erosion and elevated breakage toughness. Therefore, the material requirements are quite advanced as these structures are often subjected to high density heat fluxes and are subject to significant changes. Therefore, precise and accurate heat transfer analysis of thick-walled cylindrical FGM structures is a requirement for engineering design and production. FGMs were created as updraft protector for aerospace and various reactors as their first application. Nowadays, under the thermomechanical loading, flywheel, turbine, such as high-temperature operating environments, such as components of the machine elements began to be used in general. The use of heterogeneous materials, called FGM, has been increasing recently. FGMs: These are composite materials that consist of two components and have mechanic properties that vary depending on the location in a continuous functional structure. Thermal stress analysis has been performed in structures made of FGM, which are frequently used in engineering structures (such as cylindrical containers, circular discs, pressure vessels, beams and hollow spheres)[1-4]. Although there have been many studies on the analysis of isotropic and laminated composite beams (i.e., [5-9]), however, the research effort dedicated to stability analysis of rectangular of FG plates has been very limited.

The numerical and exact solutions of thermo-elastic analysis of FG rotating disks have submitted by Arnab et al. [10]. Zenkour [11] examined the effect of gradient grading on FG rotating solid disks on radial displacement and stresses in a sandwich structure. Çallıoğlu et al. [12] calculated thermal stresses by combining the high level shear deformation theory with multi-layer method in rotating thick-walled cylindrical containers made of FGM. Sharma et al. [13] showed tensile stress and displacement for the thin FGM disk-shaped under the influence of temperature dispersion, angular velocity and thickness. Durodola and Adlington [14] examined the effects of non-homogeneous material parameters on stresses on stress analysis on FG rotary discs (and rotors) at a certain angular velocity. Go et al. [15], using the finite element approach, have shown that a regular cutter or grinding disc with circular free force uniformity can be designed by properly controlling certain parameters to have better thermo-elastic properties. Hassani et al. [16] using Mindlin's theory, created stress distributions on FG rotary discs with nonhomogeneous thickness under thermal loads. Liew et al. [17] analyzed the thermal stresses in the FGM cylinder. Kordkheili and Naghdabadi [18] obtained a quasi-analytical resolution analysis with the centrifugal force and power law dispersal of the volume portion under volumetric thermal loads for a fine axial symmetrical rotary free wheel drive made of FGM. Based on Afsar and Go [19], 2-D thermoelastic theories, the FGM rotating disc with radial direction exponentially varying material properties exposed to combined thermal and centrifugal load was investigated. Peng and Li [20] have developed an efficient method by transforming the thermo-elastic behavior of the FGM disc, whose material properties arbitrarily changing radial way, into Fredholm integral equations. The effects of the gradient considering both the law of power and radial homogeneity on the stress dispersion in FGM rotary solid disks have investigated through Peng and Li [21]. Naghdabadi and Kordkheili [22] obtained using a finite element method for thermo-elastic analysis of FG number plates and crusts. You et al. [23] are utilized a Runge-Kutta mathematical solution technique for elastoplastic stresses on revolving discs of varying thickness and density. A design of the thermo-elastic load-dependent FGM disc designed with load optimization is proposed by Khorsand and Tang [24].

This paper, the evaluation of hollow FGM discs subject to linearly rising temperature dispersion, with the boundary conditions, is reproduced by deriving radial, tangential, equivalent stresses and radial displacement equations. Two different functions form such as power-law, exponential with free state(fr-f) and fixed–free(fx-f) boundary conditions are applied for the governing equation. The differential equations obtained mathematically in the space coordinate system consist mostly of variable coefficients. Thus, this situation indicates the two-point boundary value problem. This article, the complementary functions method (CFM), which is an effective analysis procedure [1, 25-27] as a starting-worth problem, which can be resolved by traditional procedures in the current written works, is used. In this study, fourth grade Runga-Kutta (RK4) method was used. The main of the Runge-Kutta method is easy to apply, provides better precision in numerical approximation cases, and process dynamics can be solved efficiently with solid differential equation models. Analytical benchmarking solutions for a homogeneous disk are utilized to verify outcomes and to observe the merging of numerical resolutions. In the current process, the place of the collocation points can be selected randomly. The major aim of this research is to show an effective and correct resolution technique. CFM is an effective and basic resolution procedure with a theoretic background in the written works [28, 29] The technique is effectively employed to structures such as curved rods [30], composite beams [31], cylinders [32, 33], spheres [34] and annular fin [35, 36] with different structural mechanical problems.

2. Formulation of Thermal Elastic Solution of the Disk

The equilibrium differential equation for the plane stress state for thick wall hollow circular disks is expressed in the form below.

$$r_i \leq r \leq r_o \qquad \frac{d(\sigma_r)}{dr} - \frac{(\sigma_r - \sigma_\theta)}{r} = 0 \tag{1}$$

where inside radius r_i, outside radius r_o, radial stress σ_r and circumferential stress are σ_θ. Tangential σ_r and radial stresses σ_θ can be written in terms of Airy stress function F

$$\sigma_\theta = \frac{dF}{dr} \qquad \sigma_r = \frac{F}{r} \tag{2}$$

The relationships between strains and stresses occurring in an FGM disk in the impact of temperature for elastic materials can be explained by Hooke's law.

$$\varepsilon_r = \frac{1}{E(r)}(\sigma_r - v\sigma_\theta) + \alpha(r)T(r) \tag{3}$$

$$\varepsilon_\theta = \frac{1}{E(r)}(\sigma_\theta - v\sigma_r) + \alpha(r)T(r) \tag{4}$$

where $T(r)$ is the size of the temperature distribution (Eq. 5) , v is Poisson's rate, $E(r)$ is elasticity modulus and $\alpha(r)$ is varying thermal growth coefficient. Elasticity modulus and thermal growth coefficient were used as power function (Pwr) (Eq. 6) and as exponential function (Exp) (Eq. 7) of radial direction.

$$T(r) = T_0\left(\frac{r - r_i}{r_o - r_i}\right) \tag{5}$$

$$\alpha(r)=\alpha_0\left(\frac{r}{r_o}\right)^m \qquad E(r)=E_0\left(\frac{r}{r_o}\right)^n \tag{6}$$

$$\alpha(r)=\alpha_0 e^{mr} \qquad E(r)=E_0 e^{nr} \tag{7}$$

where E_0 and α_0 are nominal elasticity modulus and thermal expansion coefficient, T_0 is ambient temperature and n, m are equivalent to nil for a homogenous disc. Strain-displacement relation are shown in Eq. 8.

$$\varepsilon_\theta=\frac{u}{r} \qquad \varepsilon_r=\frac{du}{dr} \tag{8}$$

where the radial displacement is represented by u. The deformation compatibility equation (Eq. 9) is obtained from Eq. 8.

$$\varepsilon_r=\frac{d}{dr}(r\varepsilon_\theta) \tag{9}$$

By making use of Eqs. (1), (2), (3) and (4), the equilibrium equations in Eqs. (10a) and (10b) read

$$F''-F'\left(\frac{n-1}{r}\right)-F\frac{(1-nv)}{r^2}=\frac{\left(\frac{r}{r_o}\right)^{n+m}\left[1+m\left(\frac{r_i}{r}-1\right)\right]T_0\alpha_0E_0}{r_o-r_i} \tag{10a}$$

$$F''-F'\left(n-\frac{1}{r}\right)-F\left(1-nrv\right)=\frac{(e)^{r(n+m)}\left[m(r_i-r)-1\right]T_0\alpha_0E_0}{r_o-r_i} \tag{10b}$$

Based upon von-Mises failure principle, equivalent stress is described by (Eq. 11)

$$\sigma_{vm}=\sqrt{(\sigma_r^{\,2}-\sigma_r\sigma_\theta+\sigma_\theta^{\,2})} \tag{11}$$

The boundary condition is selected as Eq. 12 (fr-f) and Eq. 13 (fx-f) depending on the inside and outside radius of the disk.

$$\sigma_r\big|_{r=r_i}=0 \quad \text{and} \quad \sigma_r\big|_{r=r_o}=0 \tag{12}$$

$$u\big|_{r=r_i}=0 \tag{13}$$

3. Numerical Solution with CFM

The constructed of the inhomogeneous governing equations were shown in Eq. 10a and Eq. 10b. Where F' expressions denote derivatives taken according to r [31]. The constructed form boundary conditions rewritten in Eq. 12 and Eq. 13.

The solution of (n)th order common differential equations by CFM [1] :

$$y(x) = y_o(x) + b_1 y_1(x) + \ldots + b_n y_n(x) \tag{14}$$

where y_o is nonhomogeneous resolution and $y_1 \ \ldots \ y_n$ are standardized solution.

The general solution of Eq. 10a and Eq. 10b in CFM over the interval [r_i, r_o] is given by

$$F(r) - F_0(r) = b_1 F_1(r) + b_2 F_2(r) \tag{15a}$$

$$F'(r) - F_0'(r) = b_1 F_1'(r) + b_2 F_2'(r) \tag{15b}$$

The CFM solutions (Eq. 15a and 15b) are calculated from GE's (Eq. 10a and Eq. 10b) using with fourth order Runge-Kutta method (RK4). Mathematical repetitions are produced in the $r_i \le r \le r_o$ variety with the footsteps of $h = 0.001$. In RK4 to get the solutions Eq. 15a and 15b, the boundary worths of governing equations (Eq. 16) are utilized variant transformation as sees

$$F' = Z_2 \qquad F = Z_1, \tag{16}$$

As a consequence of RK4, b_1 and b_2 can be obtained for fr-f (Eq. 17) and fx-f (Eq. 18) conditions as follows

$$\begin{vmatrix} F_1(r_i) & F_2(r_i) \\ F_1(r_o) & F_2(r_o) \end{vmatrix} x \begin{vmatrix} b_1 \\ b_2 \end{vmatrix} = \begin{vmatrix} -F_0(r_i) \\ -F_0(r_o) \end{vmatrix} \tag{17}$$

$$\begin{vmatrix} r_i F_1'(r_i) - vF_1(r_i) & r_i F_2'(r_i) - vF_2(r_i) \\ F_1(r_o) & F_2(r_o) \end{vmatrix} x \begin{vmatrix} b_1 \\ b_2 \end{vmatrix} = \begin{vmatrix} vF_0(r_i) - r_b F_0'(r_i) \\ -F_0(r_o) \end{vmatrix} \tag{18}$$

4. Confirmation of the Suggested Solution Program

The analytical solutions obtained using the notations of the current study to a homogeneous disc are given below. In solutions, symbolized by the modulus of elasticity E and Poisson's rate v, radial displacement is

Table 1. Collation of CFM results with analytic solutions for homogeneous disk.

r/r_0	U		σ_r		σ_θ	
	CFM	Analytic	CFM	Analytic	CFM	Analytic
0.2	0.0000000	0.0000000	0.0000000	0.0000000	-1.0000000	-1.0000000
0.3	0.0001350	0.0001350	-0.2474747	-0.2474747	-0.5479797	-0.5479797
0.4	0.0003600	0.0003600	-0.2897727	-0.2897727	-0.3011362	-0.3011362
0.5	0.0006750	0.0006750	-0.2727272	-0.2727272	-0.1136362	-0.1136362
0.6	0.0010800	0.0010800	-0.2323232	-0.2323232	0.0505052	0.0505052
0.7	0.0015750	0.0015750	-0.1808905	-0.1808905	0.2036182	0.2036182
0.8	0.0021600	0.0021600	-0.1235795	-0.1235795	0.3508525	0.3508525
0.9	0.0028350	0.0028350	-0.0628505	-0.0628505	0.4946690	0.4946690
1.0	0.0036000	0.0036000	0.0000000	0.0000000	0.6363636	0.6363636

$$U = \frac{r}{\left[\left(\frac{r_0}{r_i}\right)^2 - 1\right]\left[\frac{E(1+\nu)}{1-\nu^2}\right]} - \frac{r_0^2/r}{\left[\left(\frac{r_0}{r_i}\right)^2 - 1\right]\left[\frac{E(\nu-1)}{1-\nu^2}\right]} \tag{19}$$

Radial stress

$$\sigma_r = \frac{1-\left(\frac{r_0}{r_i}\right)^2\left(\frac{r}{r_i}\right)^{-2}}{\left(\frac{r_0}{r_i}\right)^2 - 1} \tag{20}$$

Hoop stress

$$\sigma_r = \frac{1+\left(\frac{r_0}{r_i}\right)^2\left(\frac{r}{r_i}\right)^{-2}}{\left(\frac{r_0}{r_i}\right)^2 - 1} \tag{21}$$

Table 1 is given in order to compare these results with analytical results by calculating radial and tangential stresses and radial displacement values at 9 points throughout the thickness, provided that they are collocated using the disk sizes and material properties given in Table 2.

The exact results listed in Table 1 reveal the good correctness and efficacy attained by the CFM when analyzing the findings achieved from the above analytic comparison solutions for the homogeneous disk; Calculations made only at 9 points along the thickness gave exact numerical results.

5. Numerical Results and Discussion

A hollow disk made of a FGM and Table 2 shows that disk dimensions and material properties.

Table 2. Disk dimensions and material properties

Parameter	Unit	Value
r_i	mm	20
r_o	mm	100
E_0	GPa	200
α_0	1/℃	12x10^{-6}
T_0	℃	300
v	-	0.29

Figure 1-a illustrates radial stresses in the FGM hollow disk throughout its radius caused by thermal lading for *n=0.5*, *m=0.5* used for boundary conditions of both the Pwr and Exp. The FG disk both the Pwr and Exp form for fx-f boundary conditions have smaller radial stress compared to both the Pwr and Exp form for fr-f boundary conditions. For some specific values of *n* and *m* for all boundary conditions, it has been determined that the radial stress value increases along the radius of the FGM disk.

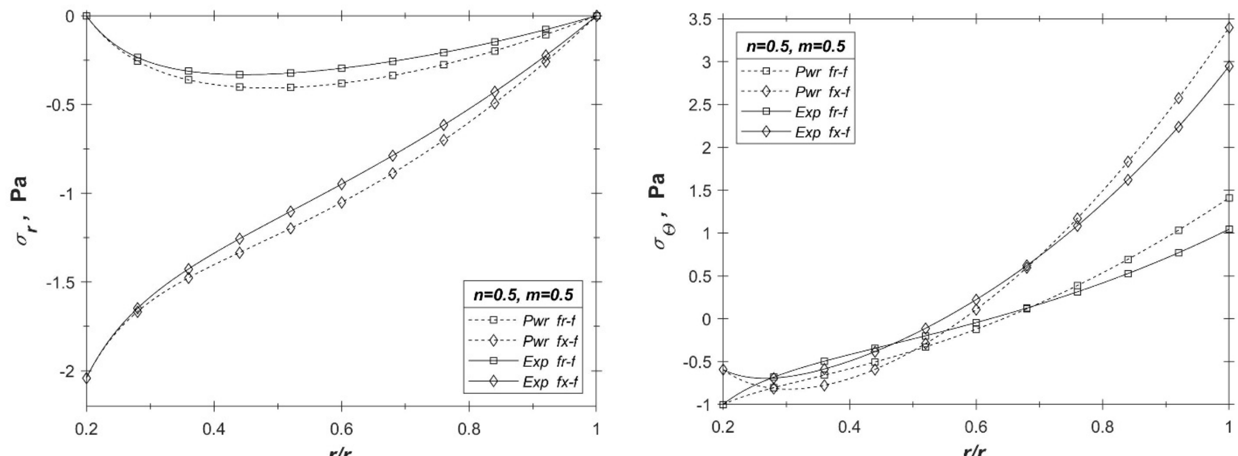

(a) (b)

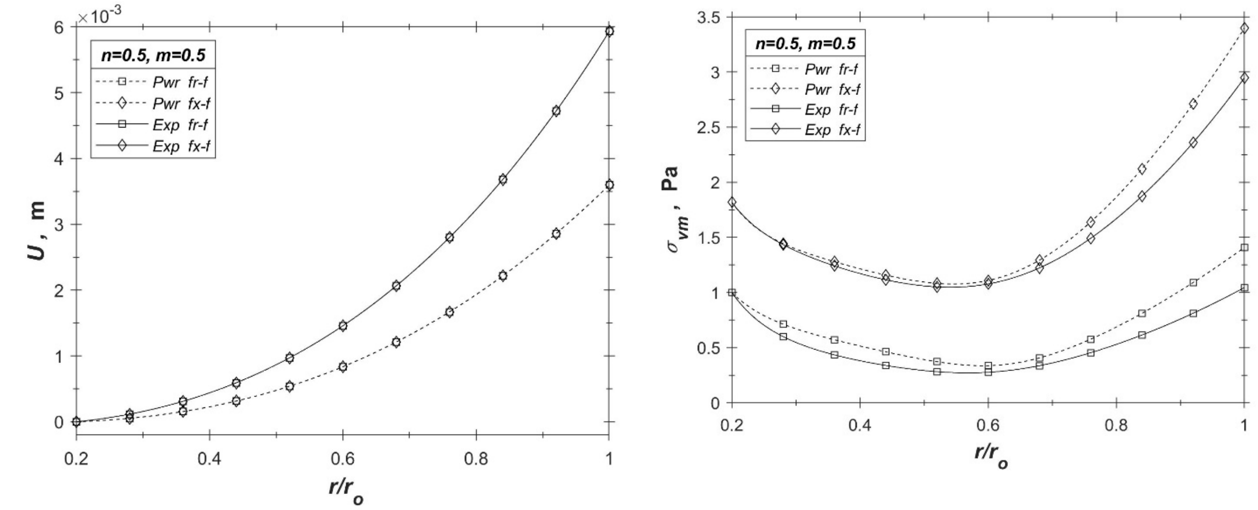

(c) **(d)**

Fig. 1. Because of the effect of temperature with the material grading and boundary conditions on the distribution of stresses and displacement in FGM hollow disk **(a)** radial stress, **(b)** hoop stress, **(c)** radial displacement and **(d)** equivalent stress.

The hoop stress dispersion caused by thermal load up for FGM hollow disk along its radius for various *n* and *m* are produced in Figure 1-b. It is noticed that for the grading mark certain values n and m for Exp form with fr-f the highest hoop stresses may not happen at the outer side. r / r_0 increases in both forms and boundary conditions while the tangential stress value increases.

The displacement FGM hollow disk with fr-f and fx-f are shown in Figure 1-c for different gradient parameter values due to thermal load. It is observed that for some particular values of the grading mark *n* and *m* (*n=0.5, m=0.5*) and all boundary conditions the displacement increases for the FGM hollow disk along its radius.

Figure 1-d explain the equivalent stress respectively for various values of n and *m*, which are the inhomogeneity parameters by considering boundary conditions of both the Pwr and Exp model for material properties FG hollow disk along its radius due to thermal loading. It can be seen from Figure 1-d that for some particular values of the grading mark n and m for all boundary conditions, equivalent stresses values decrease to the midpoint of the thickness of the thick-walled disk, the rest increases

The displacement with radial, hoop, and equivalent stresses owing to the thermal loading up along the normalized radial direction for different values of *n* in the hollow disc given in Figure 2. Thus, radial stresses (a) are high for the highest inhomogeneity parameter for both profiles.

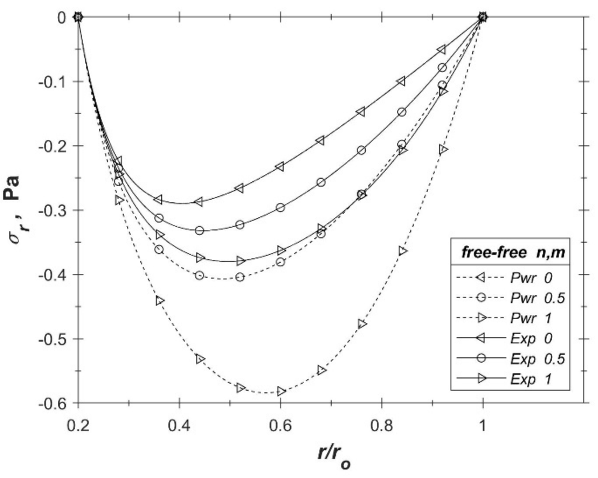

(a)

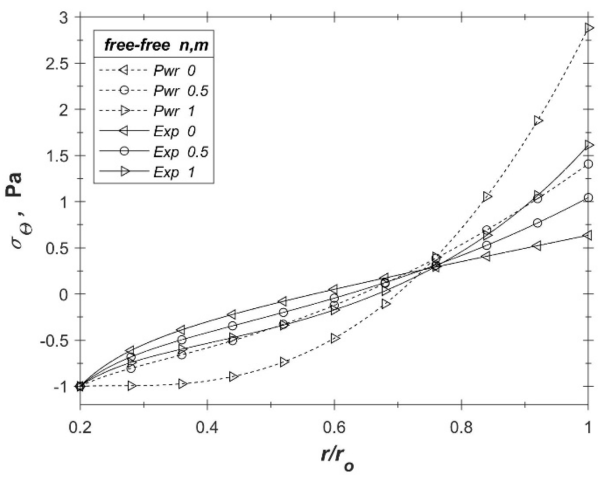

(b)

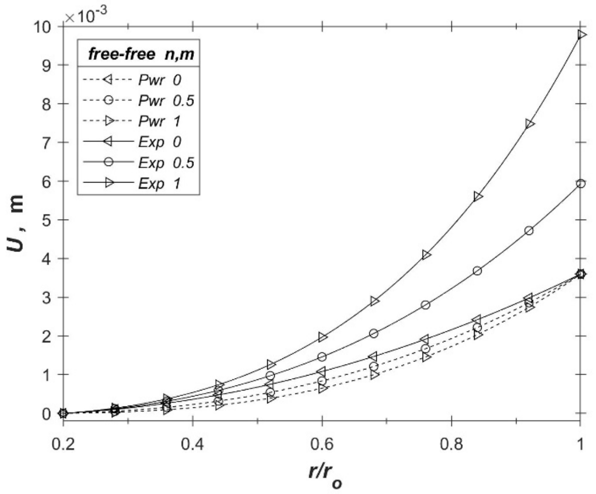

(c)

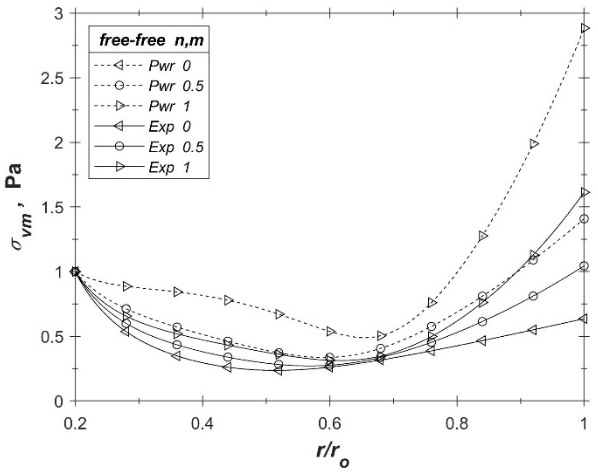

(d)

Fig. 2. Distribution of stresses and displacement in the hollow disk under the impact of temperature disk with the material grading and boundary conditions along the normalized radial direction for different values of *n, m* **(a)** radial stress, **(b)** hoop stress, **(c)** radial displacement and **(d)** equivalent stress.

It was found that for *n* and *m* used for Pwr form with fr-f the maximum hoop stresses (in the figure b) may occur at the outside side. While the hoop stress values increase, increasing the r/r_0 for all boundary conditions and both Pwr and Exp function. The increase in gradient parameter for both the Exp profile and the Pwr profile of the FG disc findings in a reduction in the radial displacement (c) value. The radial displacement values increase, increasing the r/r_0 both Pwr and Exp function. As the gradient parameters increase, the equivalent stress (d) decreases down to the midpoint of the r/r_0 while the rest increases.

Figure 3 shows the radial displacement values for radial, tangential, and equivalent stresses caused by the thermal loading in the FG disk for various gradient parameter values and variable elasticity modulus and thermal expansion coefficient profiles. Looking at this figure, it is seen in the radial stress chart (a) that the stress reduces with increasing gradient parameter for both function form types, and the stress values increase with increasing thickness.

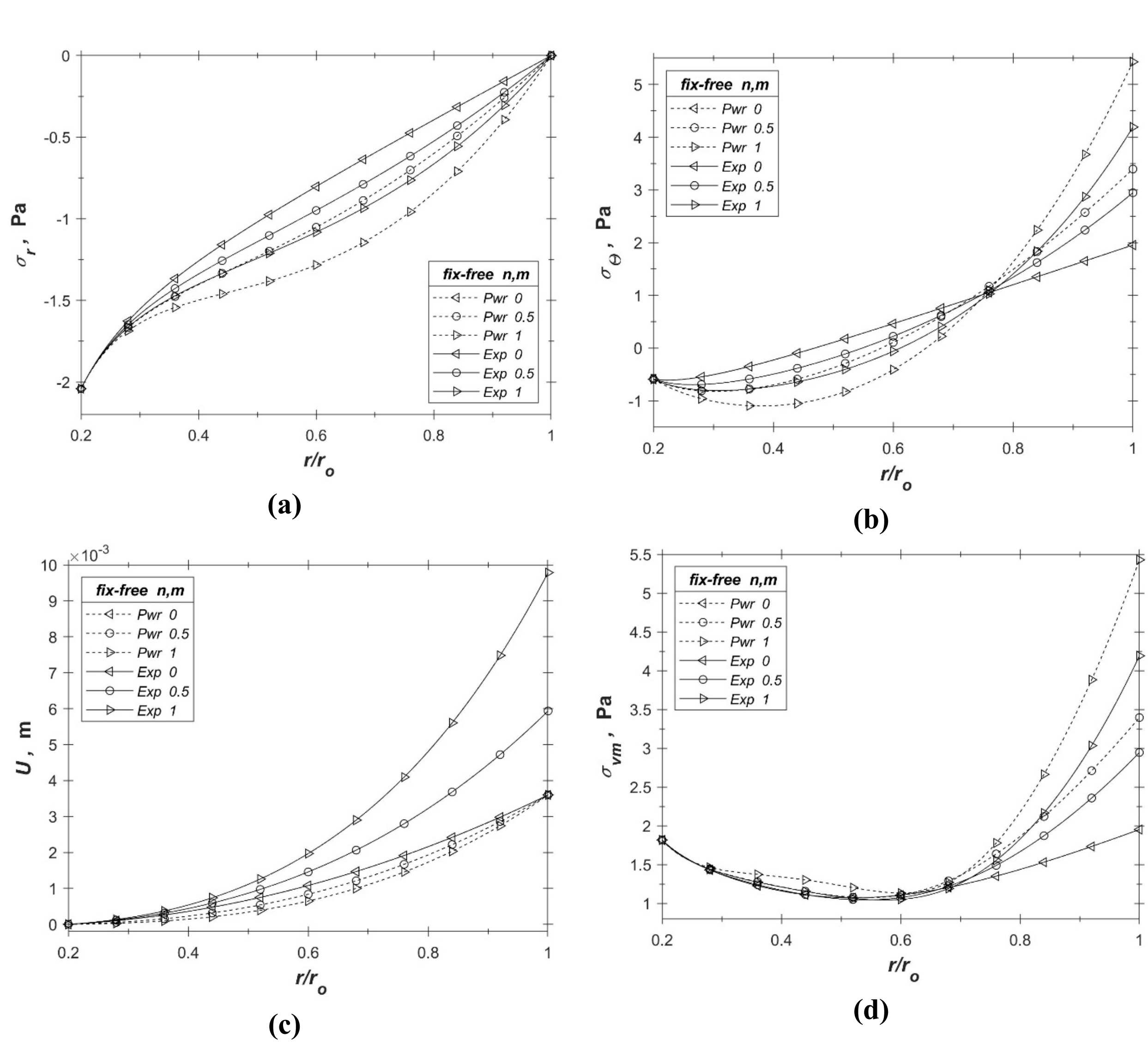

Fig. 3. In the hollow disk under the impact of temperature disk with the material grading and boundary conditions various values of the rating parameter *n ,m* **(a)** radial stress, **(b)** hoop stress, **(c)** radial displacement and **(d)** equivalent stress.

In the hoop stress graph (b), the tension value decreases with increasing gradient parameter for both profiles. However, the hoop stress values increase, increasing the r/r_0 for all boundary conditions and both Pwr and Exp. In the displacement graph (c), displacement values decrease with increasing gradient parameter for both profiles. The r/r_0 increases, and the displacement value increases for both profiles. In the equivalent tensile graph (d), as the gradient parameters increase, the equivalent stress (d) decreases down to the midpoint of the r/r_0 while the rest increases.

6. Conclusions

An examination of the hollow disk made of FGMs owing to thermo-mechanical loading is submitted. Thermo-elastic stresses are obtained for the hollow disk with both fr-f and fx-f boundary conditions. For FGM disk, modulus of elasticity and thermal growth coefficient are assumed to differ power-law and exponentially in radial way and numerical results are presented. When the numerical results in this study are evaluated, the results are briefly summarized below:

- The similar value of the *n, m* radial pressure is highest when the hollow FGM disk, the power-law function profile and the exponential function profile disk are the lowest in fr-f and fx-f boundary conditions.

- When the radial stress distribution is examined, FGM is zero on the inner and outer surfaces of the disc, although the stress stays on as tension in the central portions for the free state.

- The hoop stress components linger stressed at the inner side of the functionally graded disc and compression at the outer side for the whole profiles and gradient parameters.

- The displacement components are lower on the inner edge of the FG disc and have higher values on the outer edge.

- The equivalent tensile component has tensile values at the inner edge of the FG disk and has an increased tensile value at the outer edge while decreasing towards the middle while constant for all profiles and gradient parameters.

- Differences in strain and displacement behavior of FG disk can be observed under fr-f and fx-f boundary conditions.

- In certain applications, the influence of thermal loads is insignificant related to inertial forces but may be of equal or greater significance to others. With the solution method proposed in this study, it can help to get a solid idea for particular products. In addition, although FG disk gradient parameter is helpful before design, it can be said that it is an important parameter in determining stresses.

References

[1] Tutuncu, N. and B. Temel, A novel approach to stress analysis of pressurized FGM cylinders, disks and spheres. *Composite Structures,* 91, 385-390, 2009

[2] Jahromi, B.H., A. Ajdari, H. Nayeb-Hashemi, and A. Vaziri, Autofrettage of layered and functionally graded metal–ceramic composite vessels. *Composite structures,* 92, 1813-1822, 2010

[3] Jahromi, B.H., G. Farrahi, M. Maleki, H. Nayeb-Hashemi, and A. Vaziri, Residual stresses in autofrettaged vessel made of functionally graded material. *Engineering Structures,* 31, 2930-2935, 2009

[4] Zhong, Z. and T. Yu, Analytical solution of a cantilever functionally graded beam. *Composites Science and Technology,* 67, 481-488, 2007

[5] Arefi, M., S. Firouzeh, E.M.-R. Bidgoli, and Ö. Civalek, Analysis of Porous Micro-plates Reinforced with FG-GNPs Based on Reddy plate Theory. *Composite Structures*, 112391, 2020

[6] Civalek, Ö. and M. Avcar, Free vibration and buckling analyses of CNT reinforced laminated non-rectangular plates by discrete singular convolution method. *Engineering with Computers*, 1-33, 2020

[7] Hadji, L. and M. Avcar, Free Vibration Analysis of FG Porous Sandwich Plates under Various Boundary Conditions. 2020

[8] Jalaei, M. and Ö. Civalek, On dynamic instability of magnetically embedded viscoelastic porous FG nanobeam. *International Journal of Engineering Science,* 143, 14-32, 2019

[9] Zhang, J., S. Ullah, Y. Gao, M. Avcar, and O. Civalek, Analysis of orthotropic plates by the two-dimensional generalized FIT method. *Computers and Concrete,* 26, 421-427, 2020

[10] Arnab, B., S. Islam, A. Khalak, and A. Afsar, Finite difference solution to thermoelastic field in a thin circular FGM disk with a concentric hole. *Procedia Engineering,* 90, 193-198, 2014

[11] Zenkour, A., Stress distribution in rotating composite structures of functionally graded solid disks. *Journal of Materials Processing Technology,* 209, 3511-3517, 2009

[12] Çallıoğlu, H., M. Sayer, and E. Demir, Elastic–plastic stress analysis of rotating functionally graded discs. *Thin-Walled Structures,* 94, 38-44, 2015

[13] Sharma, J., D. Sharma, and S. Kumar, Vibration analysis of a rotating FGM thermoelastic axisymmetric circular disk using FEM. *International Journal for Computational Methods in Engineering Science and Mechanics,* 14, 262-270, 2013

[14] Durodola, J. and J. Adlington. *Functionally graded material properties for disks and rotors*. in *Key Engineering Materials*. 1997. Trans Tech Publ.

[15] Go, J., A. Afsar, and J. Song, Analysis of thermoelastic characteristics of a rotating FGM circular disk by finite element method. *Advanced Composite Materials,* 19, 197-213, 2010

[16] Hassani, A., M. Hojjati, E. Mahdavi, R. Alashti, and G. Farrahi, Thermo-mechanical analysis of rotating disks with non-uniform thickness and material properties. *International Journal of Pressure Vessels and Piping,* 98, 95-101, 2012

[17] Liew, K., S. Kitipornchai, X. Zhang, and C. Lim, Analysis of the thermal stress behaviour of functionally graded hollow circular cylinders. *International Journal of Solids and Structures,* 40, 2355-2380, 2003

[18] Kordkheili, S.H. and R. Naghdabadi, Thermoelastic analysis of a functionally graded rotating disk. *Composite Structures,* 79, 508-516, 2007

[19] Afsar, A. and J. Go, Finite element analysis of thermoelastic field in a rotating FGM circular disk. *Applied Mathematical Modelling,* 34, 3309-3320, 2010

[20] Peng, X.-l. and X.-f. Li, Thermoelastic analysis of functionally graded annulus with arbitrary gradient. *Applied Mathematics and Mechanics,* 30, 1211-1220, 2009

[21] Peng, X.-L. and X.-F. Li, Effects of gradient on stress distribution in rotating functionally graded solid disks. *Journal of Mechanical Science and Technology,* 26, 1483-1492, 2012

[22] Naghdabadi, R. and S.H. Kordkheili, A finite element formulation for analysis of functionally graded plates and shells. *Archive of applied mechanics,* 74, 375-386, 2005

[23] You, L., Y. Tang, J. Zhang, and C. Zheng, Numerical analysis of elastic–plastic rotating disks with arbitrary variable thickness and density. *International Journal of Solids and Structures,* 37, 7809-7820, 2000

[24] Khorsand, M. and Y. Tang, Design functionally graded rotating disks under thermoelastic loads: Weight optimization. *International Journal of Pressure Vessels and Piping,* 161, 33-40, 2018

[25] Aslan, T.A., A.R. Noori, and B. Temel, A unified approach for out-of-plane forced vibration of axially functionally graded circular rods. *European Mechanical Science,* 2, 37-45, 2018

[26] Celebi, K., D. Yarimpabuc, and N. Tutuncu, Free vibration analysis of functionally graded beams using complementary functions method. *Archive of Applied Mechanics,* 88, 729-739, 2018

[27] Celebi, K., D. Yarimpabuc, and T. Baran, Forced vibration analysis of inhomogeneous rods with non-uniform cross-section. *Journal of Engineering Research,* 6, 189-202, 2018

[28] Jing, L.-l., P.-j. Ming, W.-p. Zhang, L.-r. Fu, and Y.-p. Cao, Static and free vibration analysis of functionally graded beams by combination Timoshenko theory and finite volume method. *Composite structures,* 138, 192-213, 2016

[29] Khan, A.A., M. Naushad Alam, and M. Wajid, Finite element modelling for static and free vibration response of functionally graded beam. *Latin American journal of solids and structures,* 13, 690-714, 2016

[30] Roberts, S. and J. Shipman, Fundamental matrix and two-point boundary-value problems. *Journal of Optimization Theory and Applications,* 28, 77-88, 1979

[31] Agarwal, R., On the method of complementary functions for nonlinear boundary-value problems. *Journal of Optimization Theory and Applications,* 36, 139-144, 1982

[32] Yildirim, V., Free vibration analysis of non- cylindrical coil springs by combined use of the transfer matrix and the complementary functions methods. *Communications in Numerical Methods in Engineering,* 13, 487-494, 1997

[33] Celebi, K., D. Yarımpabuc, and I. Keles, A novel approach to thermal and mechanical stresses in a FGM cylinder with exponentially-varying properties. *Journal of Theoretical and Applied Mechanics,* 55, 2017

[34] Celebi, K., D. Yarimpabuc, and I. Keles, A unified method for stresses in FGM sphere with exponentially-varying properties. *Structural Engineering and Mechanics,* 57, 823-835, 2016

[35] Yıldırım, A., K. Celebi, and D. Yarımpabuç, A Practical Approach for Thermal Stress of Functionally Graded Annular Fin. *Journal of Engineering Thermophysics,* 28, 556-568, 2019

[36] Yıldırım, A., D. Yarımpabuç, and K. Celebi, Thermal stress analysis of functionally graded annular fin. *Journal of Thermal Stresses,* 42, 440-451, 2019